Flow Characterization and Redesign of Load-Leveling Valves for Improving Transient Dynamics of Heavy Truck Air Suspensions

Zebo Zhu

Thesis submitted to the faculty of the Virginia Polytechnic Institute and State University in partial fulfillment of the requirements for the degree of

Master of Science

In

Mechanical Engineering

Mehdi Ahmadian, Chair

Reza Mirzaeifar

Steve Southward

November 4, 2016

Blacksburg, VA

Keywords: Air Suspensions, Flow Characterization, Heavy Truck, Load-Leveling Valve

Flow Characterization and Redesign of Load-Leveling Valves for Improving Transient Dynamics of Heavy Truck Air Suspensions

Zebo Zhu

Abstract

This research provides a thorough flow characterization study to compare the functionality of two types of load-leveling valves that are commonly used for air suspension systems of commercial trucks. The first valve features a simple disk/slot design and is relatively compact for installation. The second type is larger and has a sophisticated, chambered design, which allows for considerably quicker fill and exhaust response times in the transient region. A new approach is introduced to estimate the transient mass flow rate of a load-leveling valve under different suspension pressures, without requiring a mass flow meter. An extensive series of dynamic tests are conducted to characterize and compare the two load-leveling valves. A generic heavy-truck pneumatic suspension, consisting of load-leveling valves, airspring, air tank, and air-hose fittings, is configured for testing. The test setup is used to evaluate the transient performance of each type of load-leveling valve in a typical truck suspension. The flow behavior of the system is validated by the force/pressure responses of the air spring due to various displacement excitations. The experimental results describe the detailed flow behavior of both valves. The flow characterization results can be incorporated as one of the most critical parameters for future model development of pneumatic systems. The tests indicate that the leveling valve with chambered design has a far faster transient flow response than the disk valve, although it is more complicated in its mechanical design and therefore costs more. To take advantage of the design simplicity of the disk valve, while also enabling it to have a faster transient response (compared with the chambered design), it is re-designed with larger flow openings and other elements to match the performance of the chambered valve for transient flow. A comparison of the experimental results and simulations validates that the re-designed rotary disk valve performs nearly the same as the chambered valve, but is simpler and costs less. The study's results are directly applicable to improving the transient dynamics of heavy truck air suspensions by providing a better understanding of how load-leveling valves can be used not only to provide ride-height control, but also to influence the roll and pitch dynamics of heavy truck.

Flow Characterization and Redesign of Load-Leveling Valves for Improving Transient Dynamics of Heavy Truck Air Suspensions

Zebo Zhu

General Audience Abstract

Heavy trucks are balanced using air suspension systems. These pneumatic controls provide stability when a truck undergoes a turn or other change in movement, including roll and pitch. As a truck experiences these changes, air is supplied or purged from the system to balance the truck. Load leveling valves control this flow of air that provides stability and are considered crucial elements in the overall design of a heavy truck. This study evaluates many different types of valves, namely a "chambered" valve and a "disk" valve. The chambered valve is large and has many parts, resulting in a heavy expense but high performance. The disk valve is a simpler design, making it much cheaper but at the expense of performance. The quality of performance that is evaluated here is the time it takes to fill or purge the air suspension, which is related to the mass flow. These characteristics were experimentally obtained and compared. The results showed the disk valve taking more time and having a lower flow rate, making its performance lower when compared to the chambered valve. The next aspect of this study is the modification of this disk valve design that is commercially available to make its performance comparable to the chambered valve. After a series of experiments, the modified design was verified to perform as well as the chambered valve. Overall, these results are important for the future design of heavy truck load leveling valves and clarify important characteristics to consider when designing them. The results from this study can lead to lower costs for heavy truck companies and a better ride for truck drivers.

Dedication

I would like to dedicate this thesis and everything I do to my beloved parents Bangbu Zhu and Shaozhi Ding. They have always been there for me during all those difficult times, especially the past nine years that I have lived in the U.S. alone. I would not be who I am here today without their love and support. I am eternally grateful.

Acknowledgements

First of all, I am extremely grateful that I can have this wonderful opportunity and privilege to work for Dr. Mehdi Ahmadian. No words can quantify the amount of respect I have for him as a young protégé. He is not only an advisor for my academic research, but also a moral mentor for life.

I would also like to thank my entire CVeSS family: Sara Vallejo, Alie Lyon, Dr. Masood Taheri, Dr. Andrew Peterson, Milad Hosseinipour, Yang Chen, Yunbo Hou, Andrew Kim, Sajjad Meymand, Ashish Jain, and Dejah Singh for their support, assistance, and guidance throughout every step of my research journey.

I am also thankful for Dr. Steve Southward and Dr. Reza Mirzaeifar's help with my project. A lot of problems that I have encountered during my research could not have been resolved without countless discussions with them.

Table of Contents

List of Figures

List of Tables

1. Introduction

In North America, a mechanical load-leveling valve which uses an arm-rod linkage to connect the truck frame and axle is the most commonly used valve in heavy truck air suspensions [1]. Load-leveling control systems need to measure the height of the current suspension in order for it to work properly. The mechanical load-leveling valve supplies or purges air from the air tank and airsprings to restore the suspension design height when the suspension moves away from the design height. The transient flow characteristic is one of the most critical parameters of the truck pneumatic suspension system because it determines the response time of the system and greatly affects the roll stability of the truck. Furthermore, mass flow rate through a load-leveling valve can be expressed in terms of a compressible fluid through an equivalent orifice area, which is always being controlled by different valve structures.

However, the valve manufacturers usually consider details of the internal structure of the load-leveling valve to be proprietary information. There are numerous papers that have modeled various air suspension systems without actually looking into the detailed interior structure of the load-leveling valves, thus, a dissection of both types of valves is performed to have a better understanding of the flow characters inside the valves. A detailed flow characterization analysis has also been carried out through these experiments. Additionally, sets of dynamic testing that coupled flow characterization setups with an airspring are conducted in order to have a more direct visual comparison of the valve performances, and also validate the results of the flow characterization tests.

This thesis presents a thorough explanation of the flow curve reshaping and redesign of the disk/slot valve process through precise metering of the orifice area and lever arm length optimization. The results showed that the transient portion of the flow characterization curves that was predicted is accurate in terms of air mass flow rate with a minimum amount of error. This level of error is inevitable considering the available dimensional tolerances in manufacturing processes, and the uncertainties of the instrumentations and experimental setups. The chambered valve's hysteresis loops are very close to the improved redesigned disk/slot valve in both the shape of the hysteresis loops and the resultant force valve.

2. Background

2.1 Pneumatic Suspension in Short

The history of pneumatic suspension began in 1847 when inventor John Lewis was granted U.S. Patent No. 4,965 for "Pneumatic Springs for Railroad Cars." However, Lewis' invention was more than 100 years ahead of the state of the art rubber technology. Pneumatic springs didn't become successful until the early 1950's, and then nylon tire cord and synthetic rubber elastomers were developed [2].

All suspension systems are defined and categorized as [3] either active, semi-active or passive systems. According to William D. Robinson [4], an active system can be defined as an automatically-controlled system (usually through an on-board electric control module) that can supply or purge controlled energy to the system to achieve performance goals. A semi-active system is one that automatically adjusts system parameters, but cannot supply controlled energy into the system. Passive air suspensions are especially competitive compared to actively or semi-actively controlled suspensions because they are simple, have fewer parts, are reliable and cost only a fraction of the active controlled suspensions.

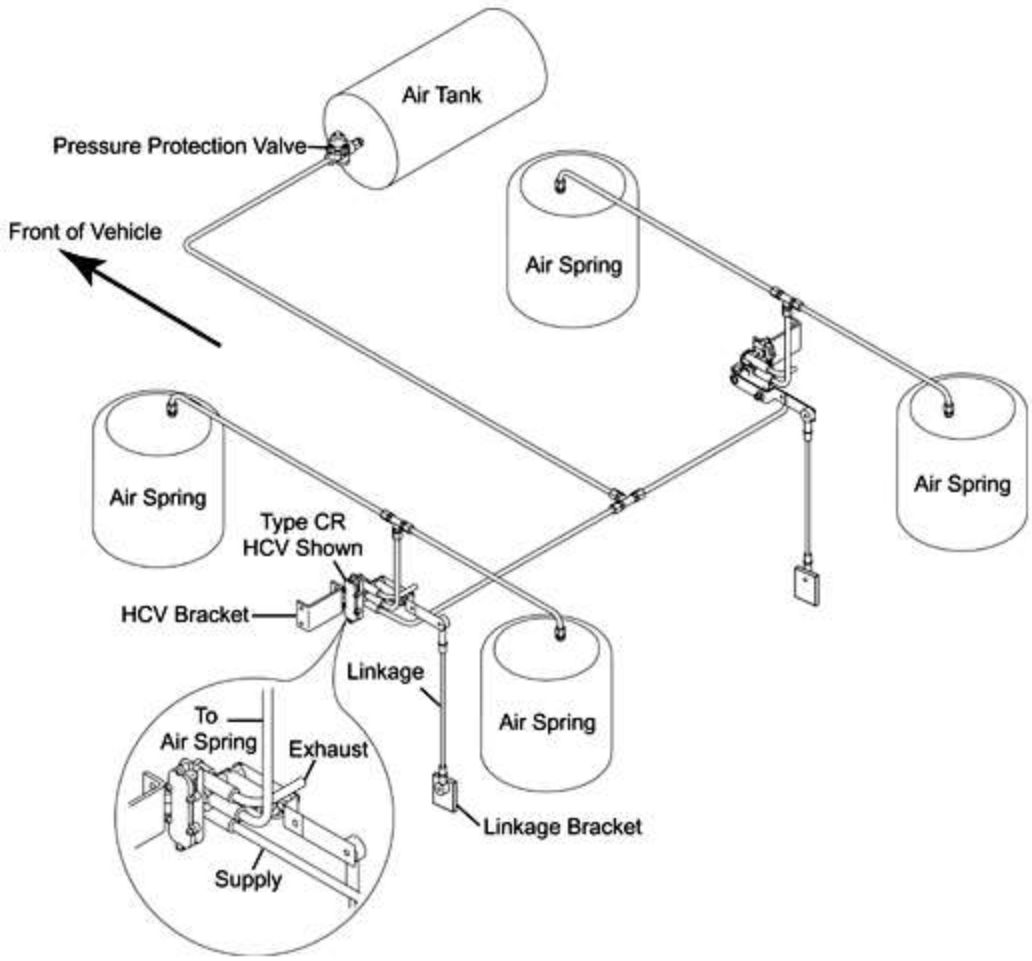

Figure 1. Pneumatic suspension schematic with a large air supply, four airsprings and a load-leveling valve [5]

The pneumatic spring is a spring that uses gas as its resilient element. This spring is often called an airspring because air is the most common gas that is utilized. The ability of the airspring to support a given load is determined by the effective cross-sectional area of the airspring and the confined gas pressure. The air inside the airspring can be compressed to the pressure required to carry the vertical load, and the compressibility of the gas provides the desired elasticity for the spring.

Furthermore, the energy storage capacity of air is much greater per unit weight than that of mechanical spring materials, such as steel coil springs. It can result in an approximately 10 times lower natural frequency for the system compared to a system that is using vibration isolators

made from steel. The airspring system is able to maintain a constant natural frequency over a wide range of load conditions by adjusting the pressure inside the airspring while keeping the same airspring static ride height [2].

The most important characteristics for almost any type of spring are load capacity, spring rate, and transmissibility. Pneumatic suspensions have the ability to carry heavy loads and variable load capacities easily by altering the air pressure inside the airsprings. They also have the ability to offer variable spring stiffness, which can be very useful in many applications. Unlike the traditional leaf or coil springs, which always have a constant spring stiffness, the stiffness of the airsprings can be modulated by changing pressures with the same height. Additionally, they have a relatively low transmissibility coefficient when compared to the steel coil or leaf springs [2].

Another advantage of the pneumatic suspension is the ability to change design height. Desired height of the air suspensions can be tuned by charging or exhausting the airsprings through connected load-leveling valve(s) and air supply. Pneumatic suspensions offer simple and inexpensive automatic leveling. Conversely, the design height of the coil or leaf spring suspensions varies with the change in load variations.

As mentioned above, the leveling control system needs to measure the height of the current suspension in order for it to work properly. In North America, a mechanical load-leveling valve which uses an arm-rod link to connect the truck frame and axle is the most commonly used [1]. The mechanical load-leveling valve supplies or purges air from the air tank and airsprings, respectively, to restore the suspension design height when the suspension moves away from the design height as shown in Figure 2. Flow characteristics are one of the most critical parameters of the truck pneumatic suspension system because they determine the response time of the system and greatly affect the roll stability of the truck.

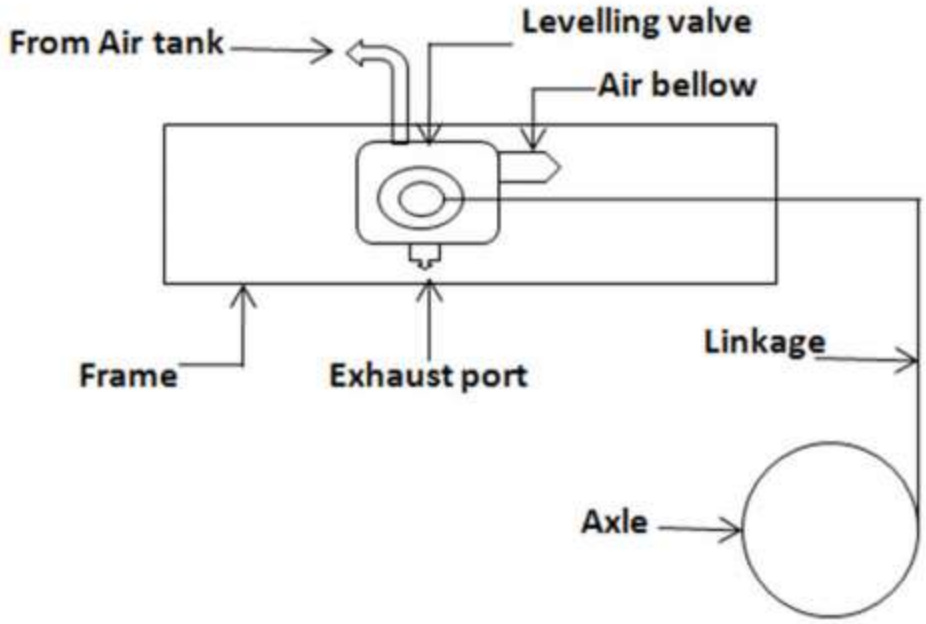

Figure 2. Sketch of a typical load-leveling valve mounted on a truck frame and connected to one of the axles [6]

2.2 Load-leveling Valves

2.2.1 Disk/Slot Valve

The first type of load-leveling valve that is the most commonly used in the heavy truck industry is the disk/slot valve that is shown in Figure 3. According to Victoria Reitz, this valve is used in roughly 70% of the air suspension systems on heavy tractor-trailer systems in North America [7]**.** The valve body itself is mounted on the truck frame, and the end of the lever arm is connected to one end of the rod. The other end of the rod is than connected to a truck axle. Through this mechanical linkage, the valve supplies air from the air tank when the same side airsprings are compressed and the distance between the truck frame and the axle is less then a permissible lower limit; the valve then purges air when the airsprings are under tension, exceeding the design distance between the truck frame and the axle [7]. The load-leveling valve is the most cirtical and also the weakest component in the pneumatic system because of its continuous use in suppling and purging air, dramatically increasing wear. Fuel consumption also increases when

excessive leakage occurs. Most importantally, the entire pneumatic system fails if the load-leveling valve fails [7].

Figure 3. The disk/slot valve is the most common valve that is used in the heavy truck industry [5]

A slot and a circular port overlap and move relative to each other as the lever arm rotates. As seen in Figure 4 and Figure 5, the orifice of the lower part uncovers slowly as the disk turns, thus allowing a ramped up/down air flow as the lever arm rotates. The disk/slot valve does not behave like other types of valves that have an undesirable full-on and full-off behavior [7]. The disk/slot valve utilizes two mirror-finished metal surfaces tightly pressed against each other to create a sealed surface. Therefore, compressed air flows directly through the orifice instead of leaking through the two contacting surfaces. According to Victoria Reitz, this disk/slot valve can handle well over 100 million cycles through testing. Nineteen tractors are installed with this type of valve through a Class 8 truck manufacturer, and zero failure reports have been received after 500,000 miles of on-road operation [7]. Moreover, this valve is able to recover from small scratches in the sealing surfaces due to the springs that are supported under the contacting surfaces; the springs can provide a strong compressive force which compensates for the material that is lost during normal wear and tear [7].

There are also a few negative aspects that make this type of valve undesirable. It has a relatively low air flow rate when compared to the other types of valves which are introduced in the

following sections. Also, the response time can be longer than the other valve types due to the construction and the physical limitations of the vale. These characteristics will be discussed in the later chapters.

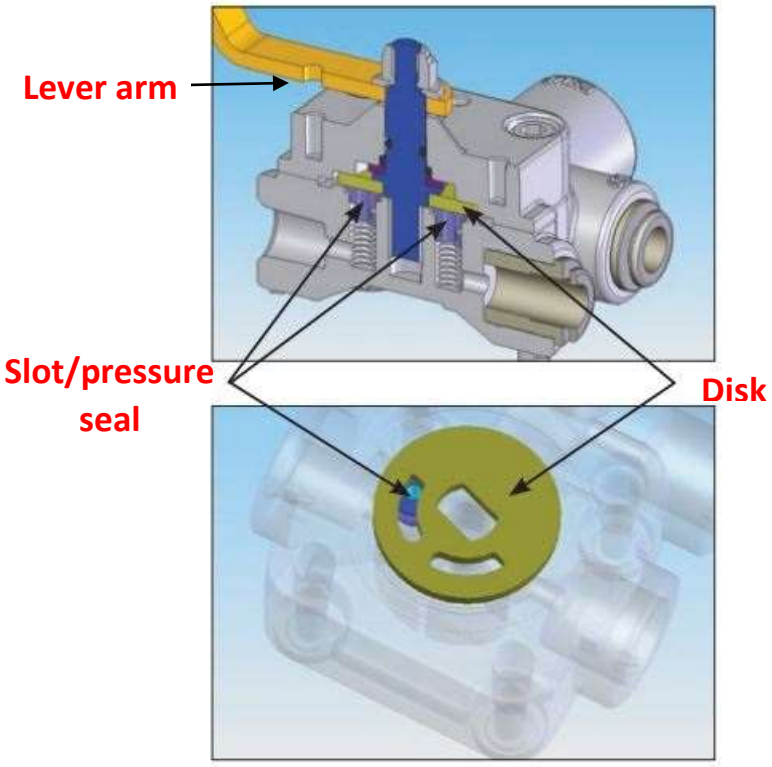

Figure 4. The interior construction of the disk/slot valve [5]

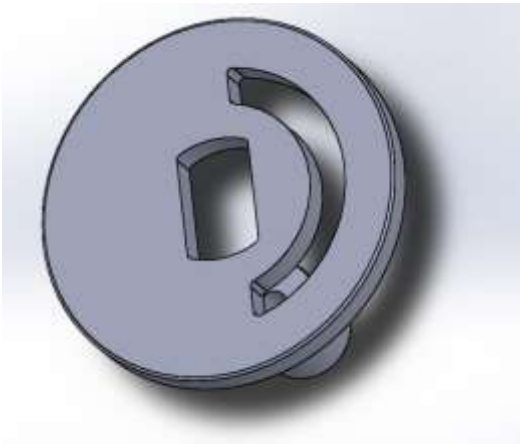

Figure 5. A detailed view of the rotating disk and the orifice hiding under the disk

2.2.2 Chambered Valve

This type of load-leveling valve has the fastest airspring fill and exhaust rates: it is up to 300% faster than any other load-leveling valve that is available in the industry. The valve and its exploded view can be seen in Figure 6 and Figure 7 below:

Figure 6. Chambered valve [8]

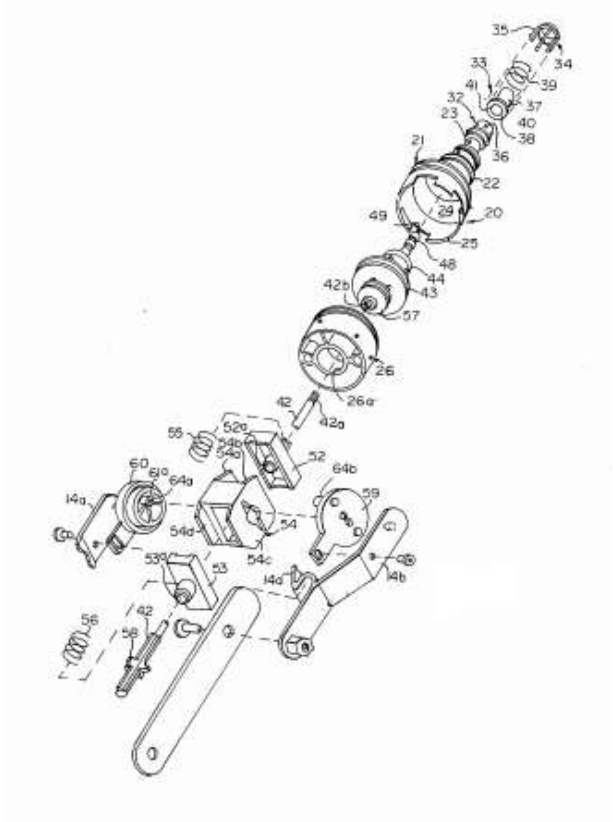

Figure 7. The exploded view of the construction of the chambered valve [9]

The inside construction of this valve contains a hollow stem with a flared tip. When the valve is in its neutral position, the elastic rubber head is fitted against the end plastic part of the inside casing in order to provide a sealing surface. The coil spring is also applying a bias against the flared tip. The hollow stem pushes the elastic rubber head off its seat when the lever arm is moving upward. There are two small thin cutouts right next to the rubber seat, which allows an accurate metered supply air flow going into the airsprings. A proposed improvement to this design could include customizing the size of the cutout if a larger or smaller supply air flow is needed. Once the rubber head is pushed past the depth of the thin cutout, the entire circumference of the seat/rubber head is then opened up. Larger air flow can be supplied into the airspring in a very short time with minimal lever arm rotation. For the purge action, when the lever arm is pulled downward, the rubber end sits on the surface of the plastic seat, and the hollow stem departs from pressing against the rubber end. The entire elastic rubber/plastic component of the valve would include an opening which allows air to pass the exhaust port when it is not blocked by the end of the hollow stem. The flared tip is a cylindrical-shaped extrusion which extends past the seal surface when the hollow stem engages the elastic rubber/plastic component. It has a precise dimension in order to create a metered flow as it is drawn away from the engagement with the elastic rubber/plastic component [9]. Therefore, the length of the extrusion determines the amount of air flowing out of the exhaust port. So if there is a load exerted on the truck frame or a sudden road input to the wheels, it changes the distance between the truck frame and the corresponding axle. The lever arm is lifted upwards and the plastic arm (shown in Figure **7**) rotates the discs; this causes the inner part of the sleeve assembly to be moved toward the right and pushes the hollow stem against the spring, which is then transferred through the piston and to the tip of the hollow stem, which pushes against the elastic rubber component. Unseating the elastic rubber/plastic component connects the supply port and the "to airspring" port, which delivers pressurized air to the airsprings and lifts the truck frame until the neutral position is achieved. Consequently, the elastic rubber component then pushes against the seat and closes off communication between all of the ports [9].

There is a time delay generated by the piston as the viscous hydraulic fluid in the chamber moves from one side of the piston to the other side through a metered hole. Thus, undesirable fluctuations are reduced by the miniature hydraulic damper. In addition, the springs that are on

top of the piston can also help to eliminate some of the undesirable fluctuations, as well as providing a means for returning the hollow stem to the neutral position [9].

However, this valve has some major disadvantages. First, the size of this chambered valve is about 2 to 3 times bigger than the disk/slot valve. Often, it is very inconvenient to have this kind of valve installed on the truck frame, both tractor and trailer, because the space in between the frames and axles is usually limited with tubes and wires, as shown in Figure 8. Therefore a custom mount (Figure 9) and brackets have to be made in order to support this valve. The mounts prepared for this thesis are made of two 8-inche long, 3 by 3, 80/20 T-slotted aluminum framing system. The mount must be at least 8 inches long due to the large size of the valve casing and the routing of the tube plumbing system. The process of making the mount is very time consuming and costly. The other disadvantage is that this valve costs nearly twice as much as the disk/slot valve. Considering the cost of the custom made parts, the price for using the chambered valve is almost three times higher than the disk/slot valve. Furthermore, the chambered valve is made of numerous parts as shown in Figure **7**; more than 20 small parts are included inside the metal housing of the chambered valve. Furthermore, a significant amount of hydraulic fluid is filled on both sides of the piston inside the hydraulic chamber which provides the time delay. All these little pieces contribute to the total cost of the valve and add complexity to the design. The more complex the design, the more likely it is to break. Having a simple design is an absolute necessity to any successful design.

Figure 8. The installation of the chambered valve requires a custom mount extended from the truck frame

Figure 9. A detailed picture of the chambered valve with the large custom-made mount

2.2.3 Piston Valve

This type of leveling valve (Figure 10) body is also mounted onto the vehicle frame and operated with the control lever arm which is linked with the axle. When the tractor/trailer is loaded or experiences a lateral acceleration, the height of the vehicle frame is too low in relation to the vehicle axle. This demands air flow from the air tank by rotating the lever arm which is connected to the tappet. This way, the piston pushes the inlet seat and the inlet is opened. Supplying air through the room between the piston and inlet components to the airspring ports, as shown in Figure 11, lifts the truck frame until the lever arm is horizontal again. Then, by providing an opposite direction lateral acceleration or unloading the tractor/trailer, the lever arm moves downward, and the arm movement transfers to the downward motion of the piston. To a point, the tip of the piston leaves the inlet seat and the orifice at the tip of the piston uncovers. This way, the pressurized air can flow out of the airsprings and into the atmosphere [10]. This valve also has a low flow rate compare to the chambered valve. Additionally, this valve is expensive compared to the disk/slot valve because it also contains many parts.

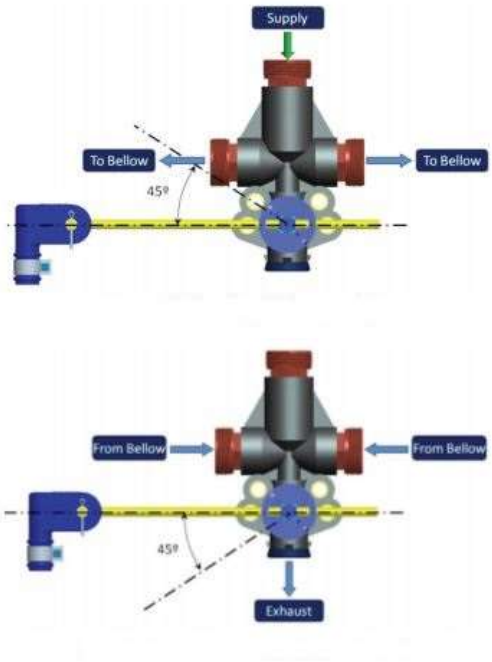

Figure 10. Piston type load-leveling valve arm operation: supply (top), purge (bottom) [10]

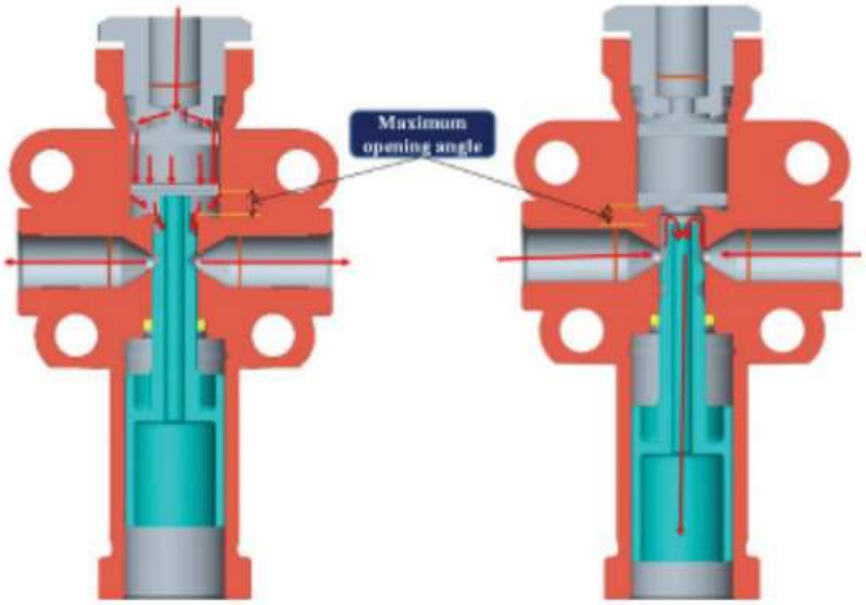

Figure 11. Flow path of the piston-type load-leveling valve (indicated in red line) [10]

2.2.4 Lever-Paddle Valve

The lever-paddle valve (as illustrated in Figure 12), has three ports: purge (top), supply (bottom), and airspring (middle). The supply and purge ports both have a valve (shown in Figure 12) with a spring-loaded release member attached to them. The valves are typically closed, and are opened to let the air flow through when release members are pressed. A paddle is secured to an actuator shaft. Rotation of the paddle in a clockwise direction, as shown in Figure 13, will cause the paddle to touch the top release member, therefore purging air through the check valve. Rotation of the paddle in a counterclockwise direction will cause the paddle to touch the bottom release member, and air will be able to be supplied through the check valve [11].

Figure 12. The exterior view of the lever-paddle valve. The top port is used for exhaust air from the airsprings, the middle port is connected to the airsprings, and the bottom port is connected to the air tank [12]

Additionally, this valve also has a damping function through a combination of vanes, holes, and hydraulic fluid. When the lever arm applies a rotation angle to the actuator shaft, the vanes moves in a counterclockwise direction, but the movement is restrained by the viscous hydraulic fluid in the chamber. A small tolerance is needed between the vanes and the damping chamber so that the viscous hydraulic fluid flows slowly around the vane from one side to the other, and therefore, the vanes will move very slowly. If the lever arm rotates for a very short duration, for

instance, with high frequency road noise, the actuator shaft will have a very small movement [11]. Therefore, this valve does not respond to short duration dynamic changes in truck frame position, thus reducing air consumption and saving fuel.

The shortcomings of this valve are very obvious: multiple rotating parts and the use of hydraulic fluid. The more complex the design, the more failure-prone it is. This valve has a shorter operating life span compare to the disk/slot design. The cost is also higher because of the complexity involved with the manufacturing process.

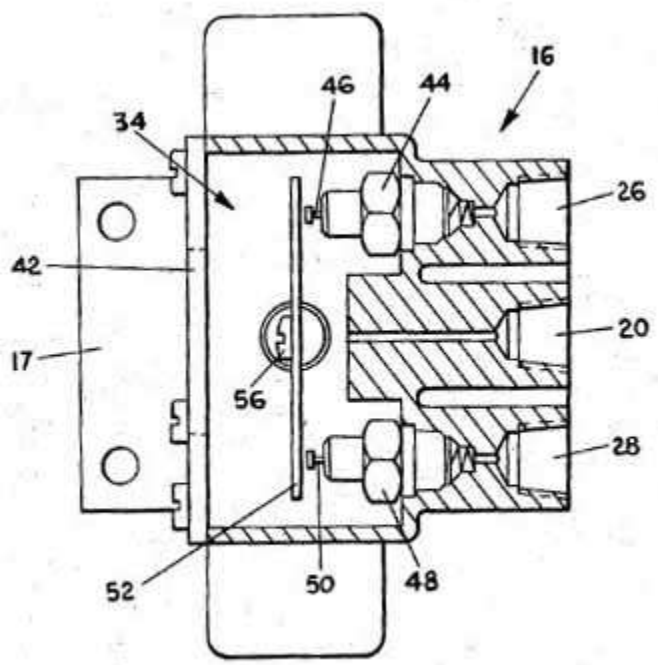

Figure 13. Section view of the three ports [11]

2.2.5 Electric Solenoid Valves

In order to use an electric solenoid valve, an electronic height control system is required. This includes several height sensors which constantly measure the distance between the truck and the axles; the collected data is then sent to the electronic control module (ECM). The collected data will change whenever the truck frame is lifted or lowered. These changes are registered by the ECM which, through the use of a solenoid valve, will automatically adjust the amount of air that

is supplied to the airsprings. This type of valve is able to provide excellent flow capability for rapid axle actuation and is electronically controlled by a solenoid, as shown in Figure 14 below:

Figure 14. Lift axle control module with a control solenoid for electric control [13]

The main problem with this type of valve is the cost, which is about six to ten times more than the mechanical valves. Therefore, more luxury passenger vehicles tend to use this kind of leveling valve; it is rarely seen on a heavy truck pneumatic suspension.

2.2.6 Advantages/Disadvantages of the Valves and the Challenges

From the details of the valves given in the previous sections, reasonable options become clear when considering cost and installation. The cheapest and the simplest design is the disk/slot valve: it only has one moving component, so it can handle millions of cycles of usage before failure. And because of the simple design and minimal parts that are used, the cost of this type of valve is also very low. Finally, it is sized so that it can easily fit under any tractor and trailer without making any custom mounts and brackets. However, it has a vital drawback, which is the relatively small flow rate when compare to other type of valves, especially the chambered valve. The chambered valve has the highest flow rate among all of the valves that have been previously

mentioned. But it is relatively expensive, and it has a larger body size, making the installation process harder than it needs to be. The goal for this thesis is to redesign the disk/slot to match the performance of the chambered valve.

Table 1. Comparisons of the advantages and disadvantages between the chambered valve and the disk/slot valve

	Chambered valve	Disk/slot valve
Advantages	▪ **Higher flow rate** ▪ **Faster response**	▪ **Only one moving part** ▪ **Smaller in size** ▪ **Lower cost**
Disadvantages	▪ **Excessive moving parts** ▪ **Larger size** ▪ **Higher cost**	▪ **Lower flow rate** ▪ **Slower response**

The challenge here is that there isn't much useful flow rate data available. In the past, many authors talked about the modeling of the pneumatic suspensions as well as the load-leveling valves. Nakajima et al. modeled the mass flow rate as a function of the opening of the valve, so the degree to which the valve opens depends on the displacement of the lever arm rotation due to the change of the car body's vertical displacement with respect to the truck frame [14]. The details of the experiment were not mentioned in this paper. Leveling valve operation and pressure regulation to the airsprings was modeled using a force actuator, which is defined with a customized function in a multi-body system model. The function senses the rotation of the lever arm angle and then actuates the force actuator corresponding to the air flow in such a way that the vehicle maintains the desired height in Sreedhar et al.'s paper [6]. Robinson et al. also modeled the mass flow rate through a valve by considering the flow of a compressible fluid through an orifice plate [4]. Airspring testing was performed in order to obtain an accurate model of the airspring and to correlate the test data to the model. However, the flow characteristics are also estimated. Moreover, flow rate across the load-leveling valve was also modeled as a function of the upstream and downstream pressures in [15], and numerous other papers also

talked about the modeling of the airsprings [16], [17]. Nieto et al. presented an analytical model of the pneumatic suspensions that is based on an experimental characterization [18]. Three components were considered: airsprings, air tank, and pipping connecting these two, but a load-leveling valve was not included. Xu et al. [19] and Bao et al. [20] generated a multi-body dynamic vehicle model in Simulink coupled with a thorough pneumatic circuit model. Kim et al. [21] and Moshchuk et al. [22] built another detailed pneumatic suspension model in AMEsin and modeled the solenoid valve by a static area-normalized mass flow equation while ignoring the dynamic properties. It appears that most publications ignored the importance of the effects of an accurate load-leveling valve. The mass flow rate of the load-leveling valve was estimated in almost every published paper. The only flow curve that is published based on the documentation of one of the valve manufacturers is that shown in Figure 15, which does not provide any useful information. For this research, the transient part of the curve is the most critical part. After contacting many of the suppliers, unfortunately, most of them consider the internal details of construction of the valve to be proprietary information, inhibiting the gathering of information about the flow rate of all of these valves that were previously explored. Therefore, the significance of having an accurate experimentally-obtained flow characterization is obvious. Also, any test results that are provided by the manufacturers should always be verified. Therefore, a flow meter or an effective method to accurately measure the flow rate is absolutely needed.

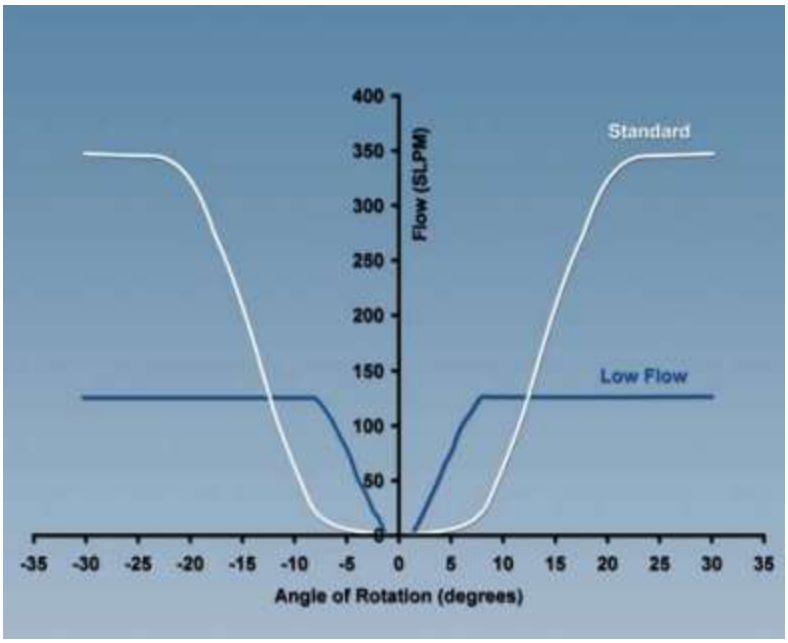

Figure 15. The only flow curve that is available on the market, but it does not provide any details of the actual characteristics of the flow [23]

Although using a flow meter would be easier, it can get very expensive for the level of accuracy needed to measure the transient flow behavior across the load-leveling valve. Most of the flow meters that are on the market are designed for measuring the flow in the quasi-equilibrium state, which means they have a relative slow response time compared to the experiments performed for this thesis. Response time is especially important in transient systems with changing environments such as pressure, temperature, magnitude, and flow rates, etc. Measurements of any parameters in transient systems are the most problematic to accurately obtain. For instance, if the dynamic measurement system being used to measure the pressure has a faster response time than the rate of change in the dynamic system, then the system can be treated as a quasi-equilibrium state. This means the measurements will be almost as accurate as those taken in the steady state system. If the measurement of the system is said to be a snap shot of what is happening in the system, then the picture will be blurred if the picture wasn't taken faster than the rate of change in the system. In a pressure measurement system, there are two factors that determine the overall measurement response: the response time of the transducer element that senses the pressure change, and the response of the interface between the transducer and the pressure. Most of pressure systems that require measurements are in quasi-equilibrium state

systems, where the system conditions are changing relatively gradually compared to the response time of the measurement system.

A good usable flow meter for this experiment would cost thousands of dollars. For example, the ultrasonic flow meter (left) [24] and thermal immersion flow meter (right) [25] that are shown in *Figure 16* below, cost $2000 to $5000+ to obtain. Even with high cost, this type of flow meter still has +/- 1 to 3% of reading accuracy. A well-designed experiment can also achieve this level of accuracy without a flow meter. The next two chapters will explain the design of experiments for flow characterization, as well as the redesign of the disk/slot valve in detail.

Figure 16. Ultrasonic flow meter (left) [24] and thermal immersion flow meter (right) [25]

3. Flow Characterization Experiments

3.1 Theory

Since an accurate mass flow meter is not practical to obtain, an alternative method to measure the flow rate across the load-leveling valve was then developed to calculate the flow rate existing the air reservoir [15].

$$\dot{m} = \frac{d(\rho_r V_r)}{dt} \qquad \text{Equation 1}$$

Equation 1 is the continuity equation where V_r is the volume of the air reservoir and ρ_r is the air density of the air inside the air reservoir, as well as the upstream air density with regards to the position of the load-leveling valve. Note that the volume of the air reservoir is constant in this case because a large fixed-volume air tank is used to represent the air tank on the truck. The only varying term is air density, so expanding Equation 1 produces

$$\dot{m} = \dot{\rho}_r V_r \qquad \text{Equation 2}$$

Also, the air density inside the reservoir at an initial equilibrium condition can be expressed as Equation 3 from the ideal gas law:

$$\rho_{r0} = \frac{P_{r0}}{RT_{r0}} \qquad \text{Equation 3}$$

where R is the specific gas constant, P_{r0} is the initial pressure of the air tank, and T_{r0} is the initial temperature inside the air tank. Assuming a constant entropy polytropic process, the expression for density at a specific state is given by:

$$\rho_r = \frac{P_{r0}}{RT_{r0}} \left(\frac{P_r}{P_{r0}}\right)^{\frac{1}{n}} \qquad \text{Equation 4}$$

where n is the polytropic exponent for air (approximately 1.4), and P_r is the instantaneous pressure of the air tank. Differentiating both sides of Equation 4 with respect to time gives

$$\dot{\rho} = \frac{1}{nRT_{r0}} \left(\frac{P_r}{P_{r0}}\right)^{\frac{1-n}{n}} \dot{P}_r \qquad \text{Equation 5}$$

Now, substituting Equation 5 into Equation 1, a first-order differential equation for mass flow rate in and out of the load-leveling valve can be obtained as follows:

$$\dot{m} = \frac{V_r}{nRT_{r0}} \left(\frac{P_r}{P_{r0}}\right)^{\frac{1-n}{n}} \dot{P}_r \qquad \text{Equation 6}$$

From the equations above, it is obvious that the mass flow rate is dependent on the rate of change and instantaneous upstream pressure of the load-leveling valve. Therefore, in order to measure the flow rate, all that is required is a pressure sensor connected upstream of the load-leveling valve.

3.2 Experimental Setup and Testing Procedure

A schematic of the flow characterization system is presented in Figure 17. The system consists of a 33-gallon air reservoir/compressor and a load-leveling valve coupled in series. To measure the supply air mass flow rate, the outlet of the air reservoir is connected to the inlet of the load-leveling valve with a Honeywell pressure transducer [26] running parallel in between to measure the upstream pressure P_r. The outlet (out to air springs) of the load-leveling valve is exposed to the atmosphere, hence the outlet pressure is approximately constant. In a realistic truck air suspension circuit, however, the upstream pressure Pr is kept constant and the downstream pressure is flexible due to different loading conditions on top of each air spring. These two configurations are technically equivalent since they all have a constant pressure side and a variable pressure side. An upward movement which is monitored by the rotary position sensor as shown in Figure 18 [27] would introduce a pressure drop on the upstream side of the load-leveling valve and is captured by the pressure transducer. A Roehrig 2K EMA electromagnetic actuator [28] is used to provide a more accurate displacement/angle input to the load-leveling valve. The actuator has a drive position resolution of 1 micron, and it is also equipped with a +/- 2000 lbs (8.8 kN) pancake-style load cell. Force, velocity, displacement and acceleration data can be stored and analyzed through Shock6 Test Control and Damper Analysis Software [29] that is provided by the actuator manufacturer. All the pressure and angle data are then collected through a data acquisition module (Data Translation DT9816) [30]. Figure 19 shows the experimental setup.

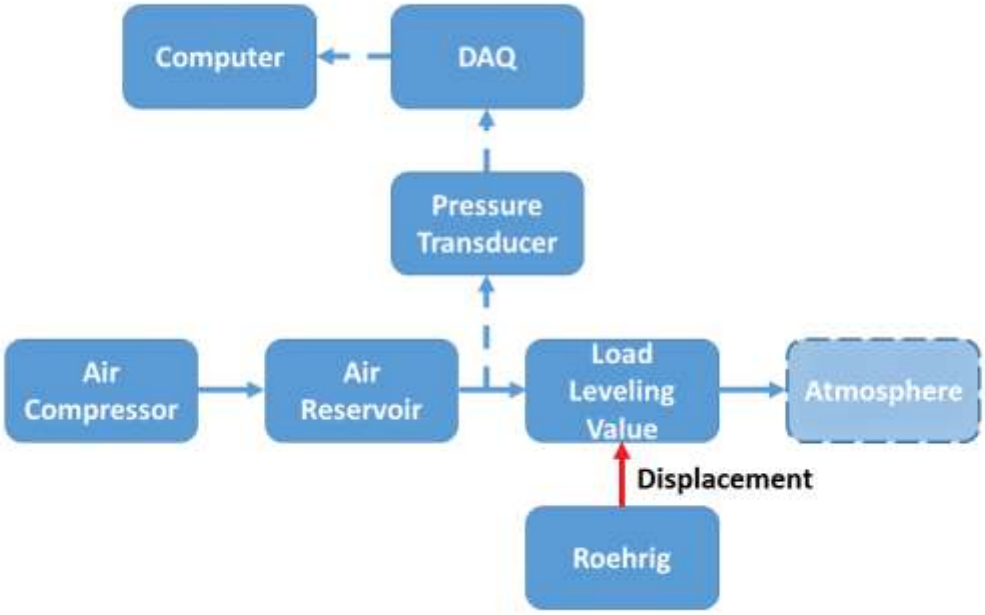

Figure 17. Schematic diagram of flow characterization test setup. Dashed lines are the representations of signals, and solid lines are the pneumatic circuit

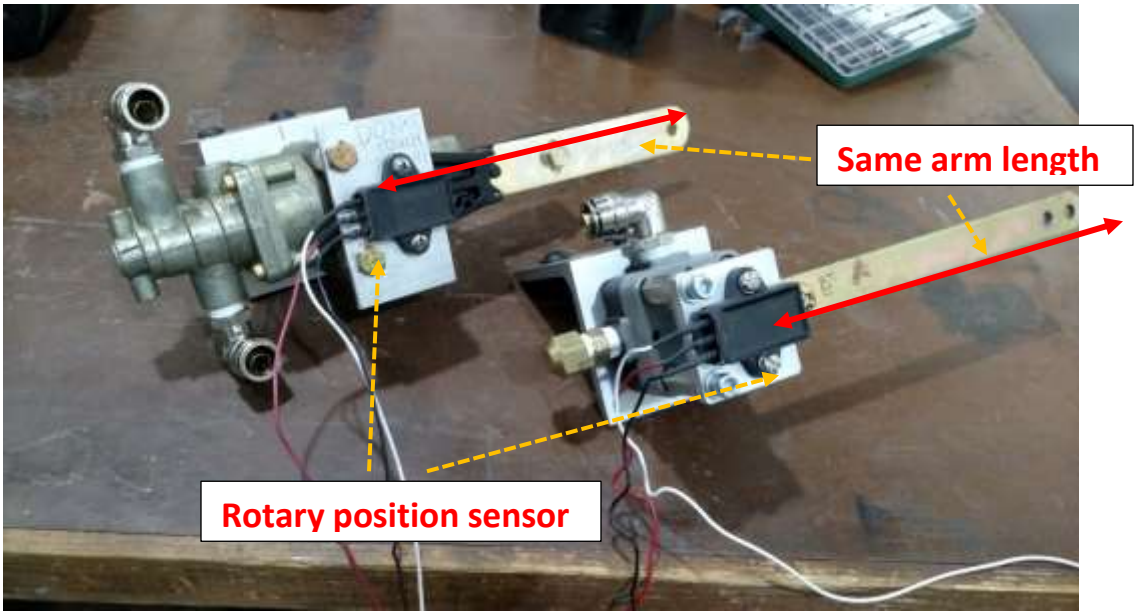

Figure 18. The instrumentation of the load-leveling valves

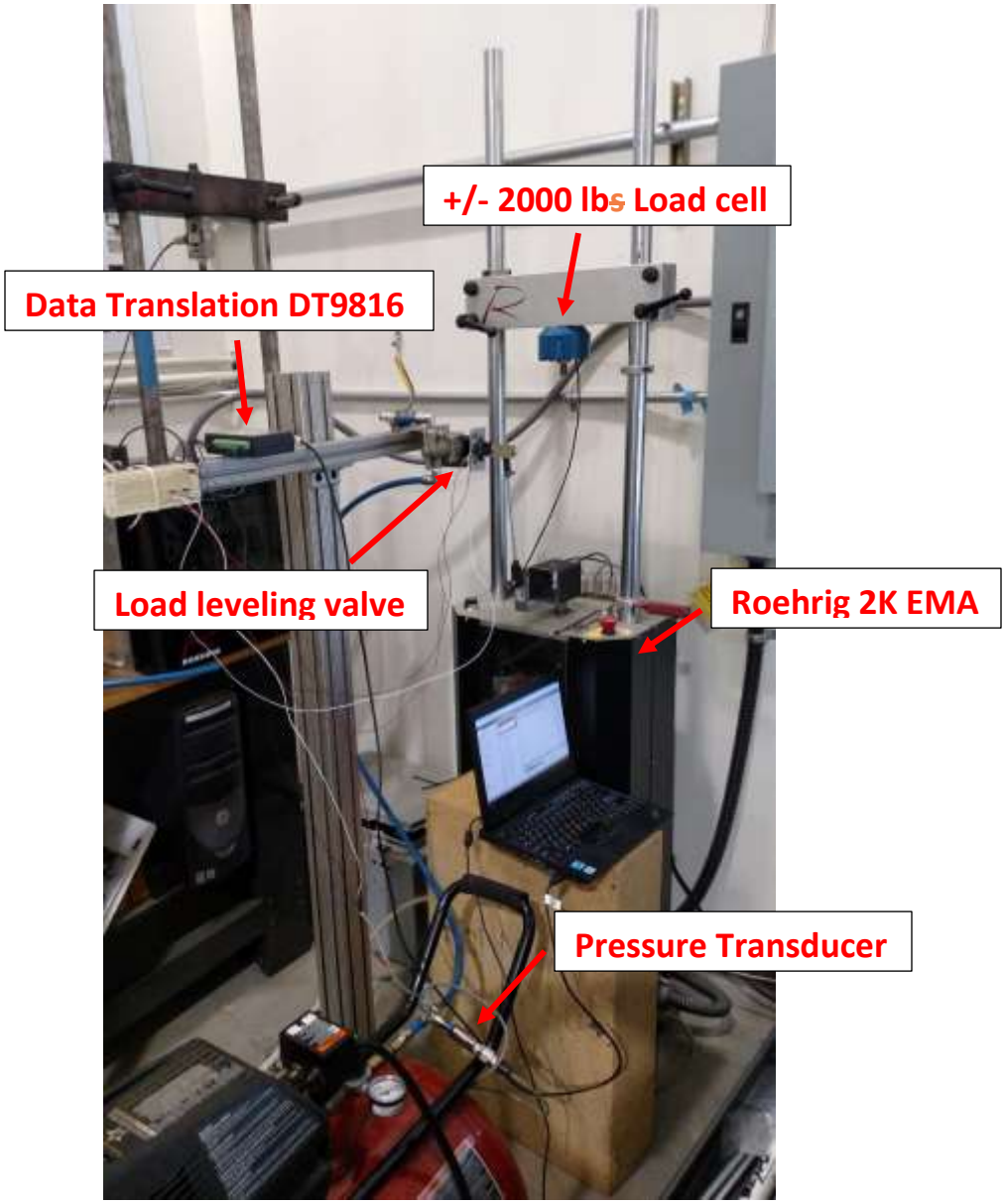

Figure 19. Flow characterization test setup

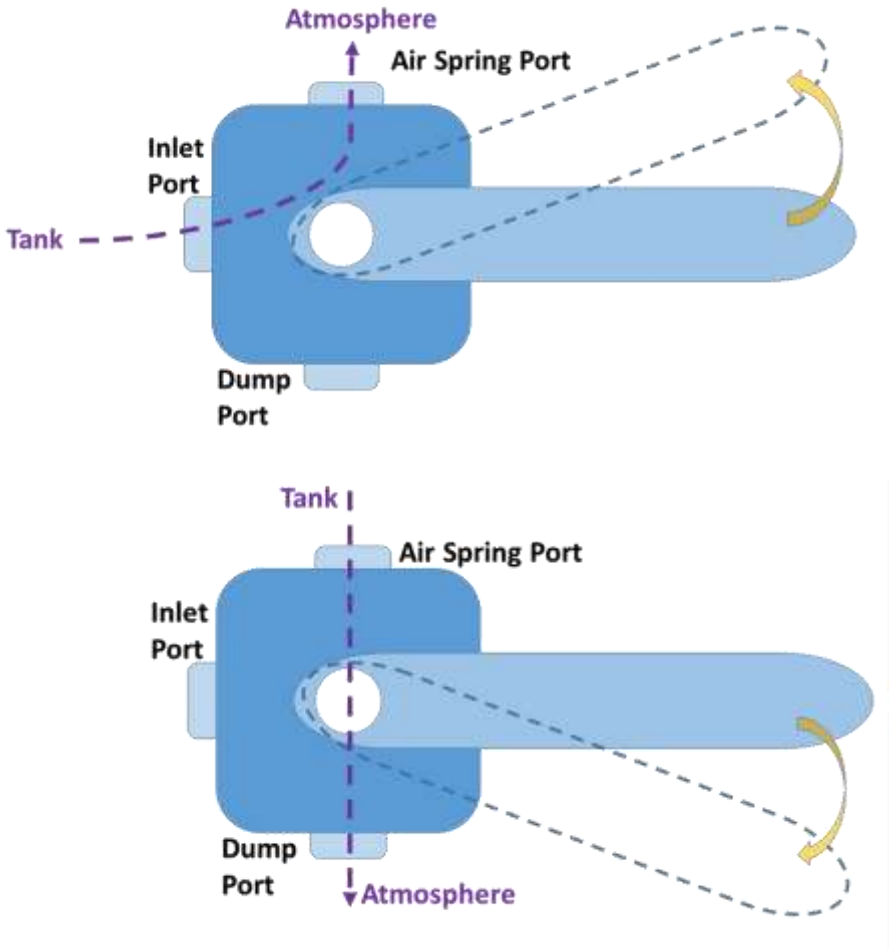

Figure 20. Flow diagram of both supply and purge tests

Conversely, shown in Figure 20, the air reservoir can also be connected to the out-to-air spring port when measuring the purge air mass flow rate. Due to the internal construction of the chambered leveling valve, the supply port needs to be sealed when performing purge tests. Air flows through the pressurized out-to-air spring port when the plunger disengages the flexible member, however, the supply port side does not have enough pressure to secure the seal surface between the flexible member and the valve seat. Hence, some air would escape from the supply port if no preventive sealing is installed. Similarly, a downward motion would lead to a pressure

drop on the upstream side. Pressure drop at various arm rotation angles was tested, however, the size of the deadband needs to be determined beforehand.

3.3 Deadband Determination

A deadband is a region of motion where the valves either do not respond to the input signal or respond at a very slow rate. The size of the deadband for the valve is intended to reduce the air consumption of the air tank while maximizing the fuel economy and the life span of the air compressor. Insignificant fluctuations due to a normal road profile won't be able to turn on the compressor, thus minimizing the allowed drift in the suspension height [1]. To achieve a relatively accurate determination of the deadband region in the lab, the Roehrig actuator is connected to the bottom of the leveling valve rod and it moves at a very slow speed. A few speeds are tested, with results indicating that 0.0025 in/sec would provide a clean figure with an exact location of where the pressure starts to drop. All of the pressure transducers and the displacements are sampled at 1000 Hz. Therefore, the measurement system being used to measure the pressure and displacement has a faster response time than the rate of change of the system pressure, so the measured system can be treated as a quasi-equilibrium state. The lower deadband determination plot for the chambered valve is shown in Figure 21, and indicates that the pressure starts to drop at an arm angle of rotation about -1.141 degrees. Table 2 lists all the measured deadbands for both types of valves.

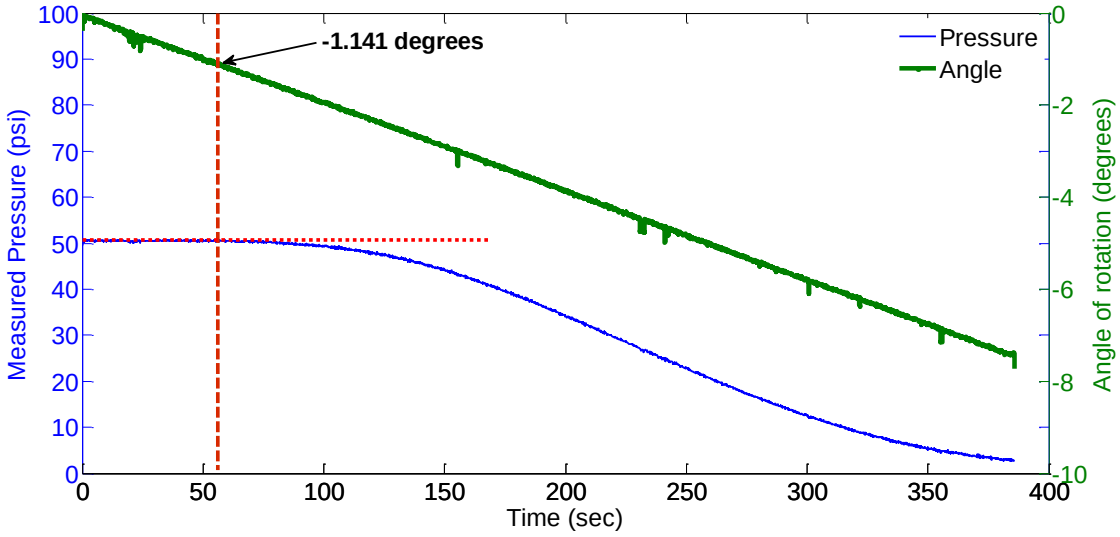

Figure 21. Plot for lower deadband determination of the chambered valve

Table 2. Experimentally obtained deadband data

	Angle (degrees)
Upper deadband (chambered)	1.17
Lower deadband (chambered)	-1.14
Upper deadband (rotor/slot)	2
Lower deadband (rotor/slot)	-2

3.4 Flow Characterization Testing

A sample upstream pressure drop at a 7˚ angle of rotation for the chambered valve is shown in Figure 22. A Roehrig actuator is connected to the bottom of the load-leveling valve's rod in order to simulate real truck axle movements. A displacement input from the Roehrig actuator is then directly propagated through the rod-arm mechanism to the rotation angle of the leveling valve. This configuration is especially important when performing dynamic tests. The air spring is attached between the bottom of the rod and the fixed cross bar on top of the Roehrig actuator. For the test data that is shown in Figure 22, an initial tank pressure of 75 psig is set before the test begins. A displacement input of 0.88 inch is sent to the rod, which is in turn translated to the angle of rotation of 7˚ to the actual valve because the lever arm length is 7.25 inches long. Note that the length of both of the valves needs to be identical (7.25 inches) in order to have a fair comparison between them. All the pressure and corresponding angle data are recorded for a time-span of 75 seconds. The raw pressure data looks noisy, but a clear trend can be traced using a third-order low-pass Butterworth filter. A few other filters have also been tested but they all have some form of phase shift with respect to the original data. The Butterworth filter that is used here does not completely reject the unwanted frequencies, but has uniform sensitivity for

the wanted frequencies. The filtered data is plotted on top of the raw signal and they seem to have a fairly good agreement. A sample mass flow rate vs. filtered pressure data can also be seen in Figure 23.

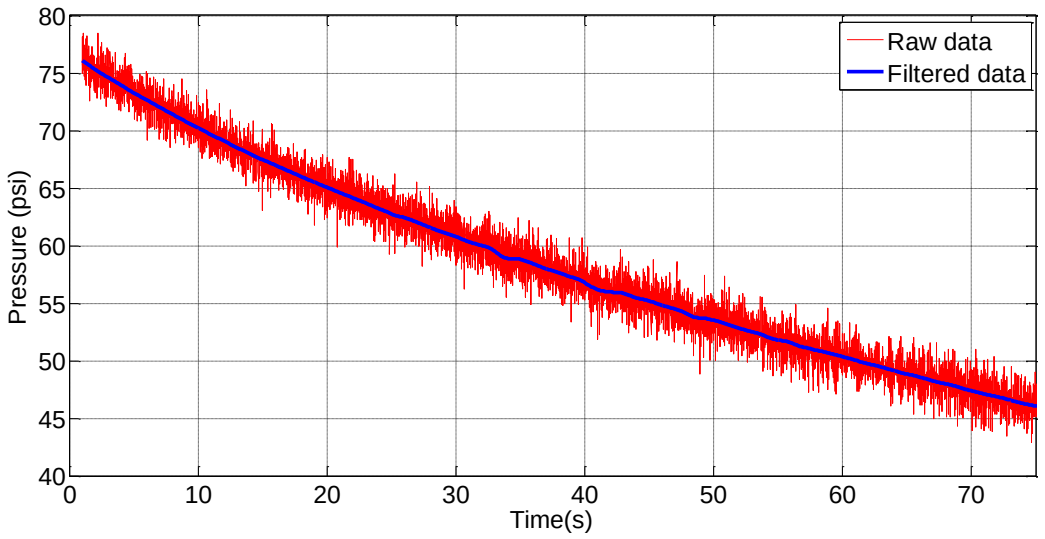

Figure 22. Sample measured raw pressure data (red) and the filtered pressure data (blue) at 7˚ angle of rotation for the chambered valve

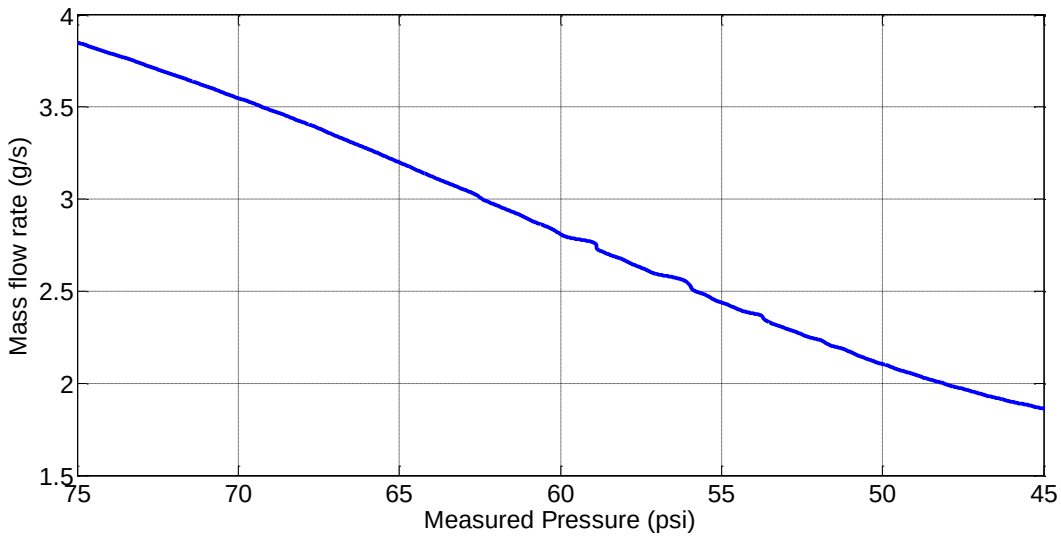

Figure 23. Sample Mass flow rate vs. filtered pressure data at 7˚ angle of rotation for the chambered valve

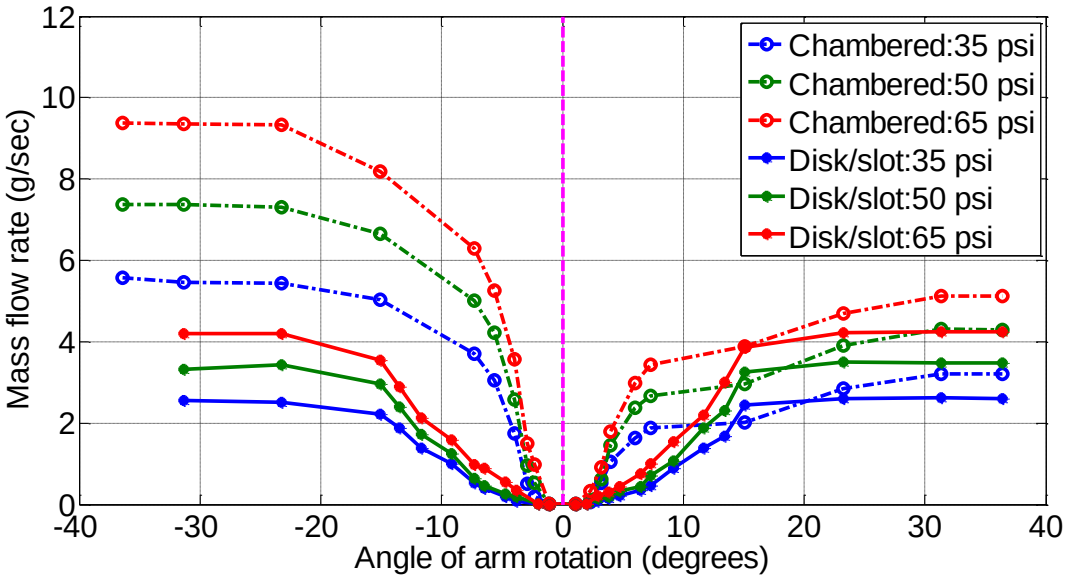

Figure 24. Flow characterization curves of both chambered and disk/slot valves

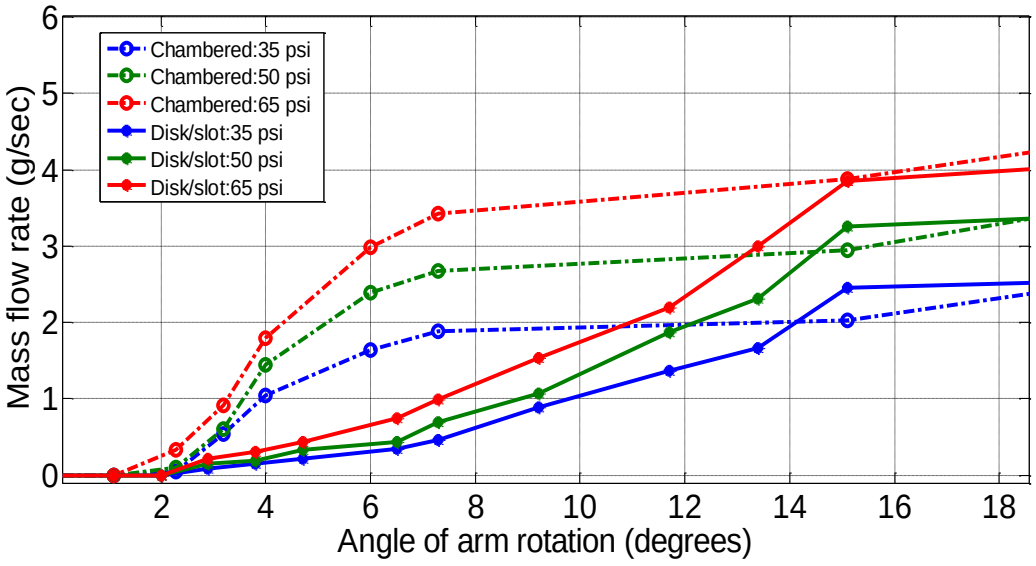

Figure 25. A close look at the transient portion of the flow characterization curves shows a large difference between these two valves

As one can observe from Figure 24 and Figure 25 above, the flow rate of the chambered valves is roughly four times higher than the disk/slot design in the transient region. In this region, air mass flow rate changes dramatically with little change to the arm rotation angle: they all leveled up at about 20 degrees of rotation on both the supply and purge sides. This angle is equivalent to about two and a half inches of suspension deflection. The goal of this study is to improve the air

mass flow rate in this transient area. Furthermore, this air flow characterization curve is later incorporated as one of the most critical parameters for the AMESim pneumatic model that is developed by Yang Chen. This model also can be coupled with TruckSim to effectively evaluate the transient dynamics of heavy truck air suspensions [31].

3.5 Dynamic Airspring Verification Testing

In order to validate the results of flow characterization experiments and have a more direct visual comparison of the valve performances on the airsprings, a secondary verification process is also needed. As shown in Figure 26, two pressure transducers are used to measure both the upstream and downstream pressure regarding the position of the load-leveling valve. Any movement of the leveling arm would be recorded by the rotary position sensor. A Roehrig 2K EMA electromagnetic actuator is also needed to provide customizable displacement inputs and frequencies to the leveling arm. Force and displacement data are stored and analyzed through Shock6 Test Control and Damper Analysis Software. All the pressure and angle data are then collected through Data Translation DT9816. A testing schematic diagram and a picture of the testing setup are shown in Figure 26 and Figure 27 below.

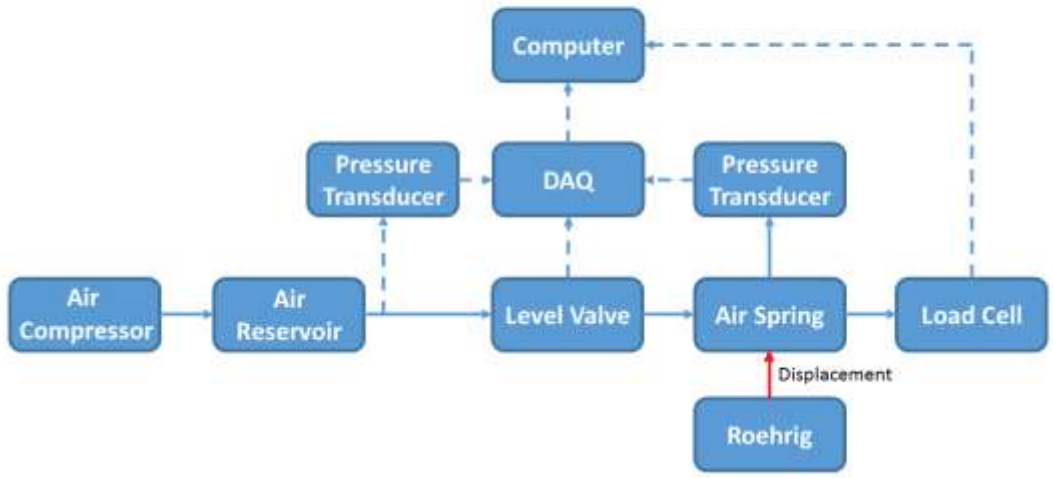

Figure 26. Schematic diagram of the airspring verification test setup. Dashed lines are the representations of signals, and solid lines are the pneumatic circuit

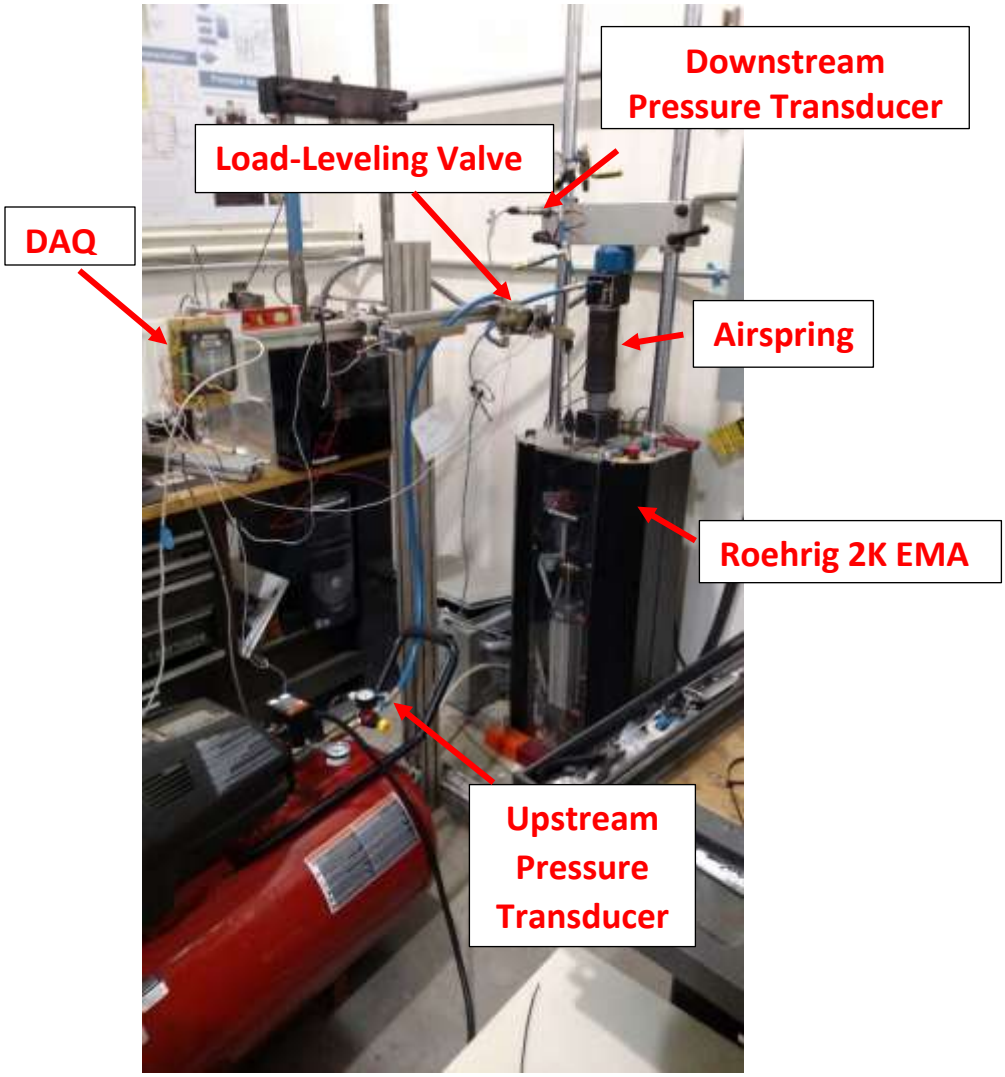

Figure 27. Airspring verification test setup

To accurately measure all the pressures, all the pressure transducers are hand-calibrated with two National Institute of Standards and Technology (NIST) certified pressure gauges. Due to the excessive vibrations from the air compressor, as well as the vibrations caused by the high pressure air flow rushing through all the pressure gauges, a liquid-filled, NIST-certified pressure gauge is also used in all of these experiments. For situations prone to vibration, a liquid-filled dial would suppress needle flutter for a more accurate reading. A liquid-filled dial gauge should also be able to absorb some of the shocks that come from pressure spikes, which may prevent damage to the gauge. The smallest tic mark on these gauges is 1 psi, so the instrument uncertainty is ½ psi for all of the following experiments as shown in Figure 28.

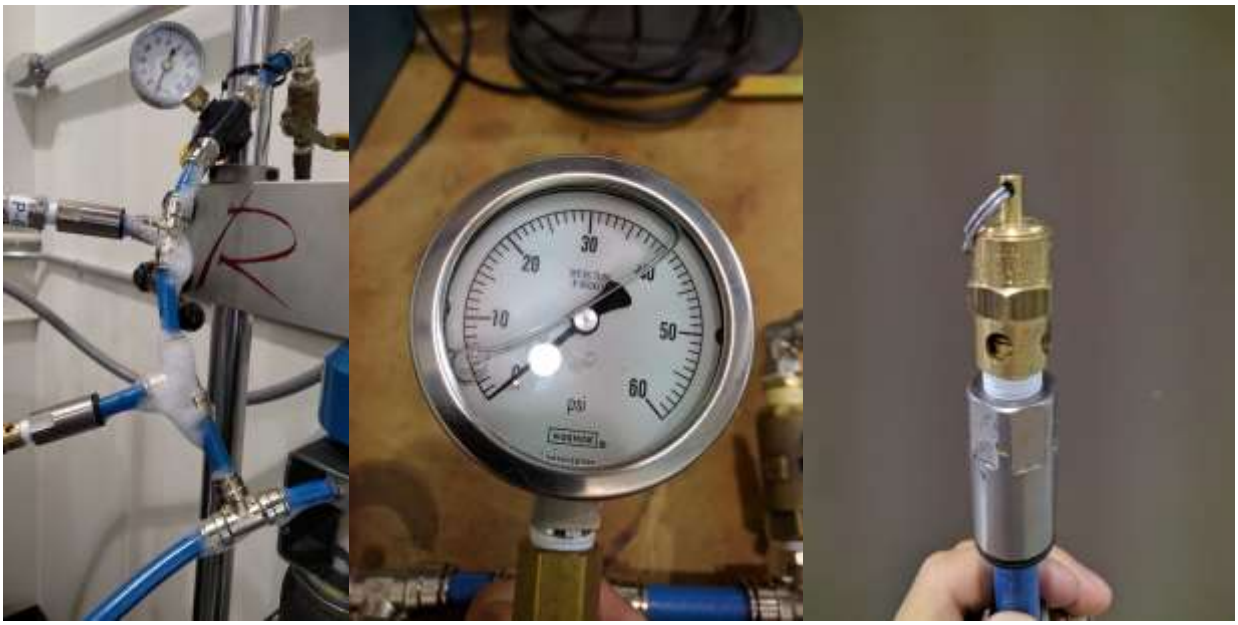

Figure 28. A pressure relief valve is placed in line with a pressure transducer, and a liquid-filled NIST-calibrated pressure gauge ensures the accuracy and safety of airspring testing. A soap test is also performed on every single connection.

Twelve sets of experiments are conducted using four different sinusoidal input displacement frequencies of 0.25 Hz, 0.5 Hz, 1 Hz, and 2 Hz, coupled with three different amplitudes of 0.5 in, 1 in, and 1.5 in. All possible combinations are tested with the purpose of mimicking the actual semi-truck suspension deflections. The pressure differential is set to 40 psi, with an upstream pressure of 60 psi and a downstream pressure of 20 psi. As shown in Figure 29 and Figure 30, zero displacement is where the initial position is before any input from Roehrig. Positive displacement values indicate that the airspring is under rebound; conversely, negative displacement values indicate that the airspring is under jounce motion. The hysteresis of a displacement-force cycle in the experiment shows that the dynamic stiffness changes when the excitation displacement changes. In both Figure 29 and Figure 30, a similar dynamic trend is observed for displacement inputs under 0.3 in, which translated to approximately 2.5 degrees of arm rotation. Dynamic stiffness of the airspring in line with the chambered valve started to increase dramatically right at about 0.3 in of displacement input. The difference of the dynamic stiffness is especially obvious in the range of 0.3 to 1.5 in of displacement (2.5 to 12 degrees of arm rotation). Referring back to the flow characterization curve in the previous chapter, air mass

flow rates of the two valves are relatively close to each other at a very small arm rotation angle (less than 3 degrees). The difference becomes larger and larger in the range of 3 to 8 degrees, and then starts to converge between 8 to 15 degrees. This analysis verified the accuracy of the supply side of the flow characterization curve. Now let's focus on the curves after the displacement inputs reach the top points of the rebound motion. From this point, the Roehrig is giving a backward displacement, but is still relatively positive regarding the starting position of this test. Therefore, the airspring is still under compression, and the leveling arm still has a positive angle of rotation, hence, the air tank is still pumping air into the airspring. That is why a backward force growth at a slower rate is observed in the figures below. It makes perfect sense that the airspring undertakes more force when the curves cross the zero displacement compare to the original starting position. According to the flow characterization curve, the air purge rate is much higher than the supply rate for the chambered valve. This behavior can be observed from the figures below. The end point force value of the chambered valve is always lower than the starting position. This is due to the higher purge rate of the chambered valve. On the other hand, the ending point force valve for the disk/slot valve is actually a little higher than the starting point, but this is not because the disk/slot valve also has a higher purge rate. The flow characterization curve clearly shows that the disk/slot valve has a relative symmetric mass flow rate for both supply and purge. The main reason could be due to the fact that the airspring area change and volume change become primary deciding factors in the force value determination. For a small displacement amplitude and relative higher frequency input, the disk/slot valve's orifice does not have a large opening, so the pressure of the airspring does not change much, hence, the effect of the pressure term inside force calculation is relatively small compared to the effect of the area change. Another possible cause could be human error, in that the neutral position may not have been set to the exact zero degree angle. Finding the exact zero angle is always a difficult task because a tiny fluctuation could result in a large discrepancy in terms of pressure measurement of the airspring. The neutral position during this set of experiments could have been set to a slightly negative degree, but this small error can be tolerated since the main goal was to observe the general trend/shapes of these hysteresis in order to verify results from the flow characterization experiments.

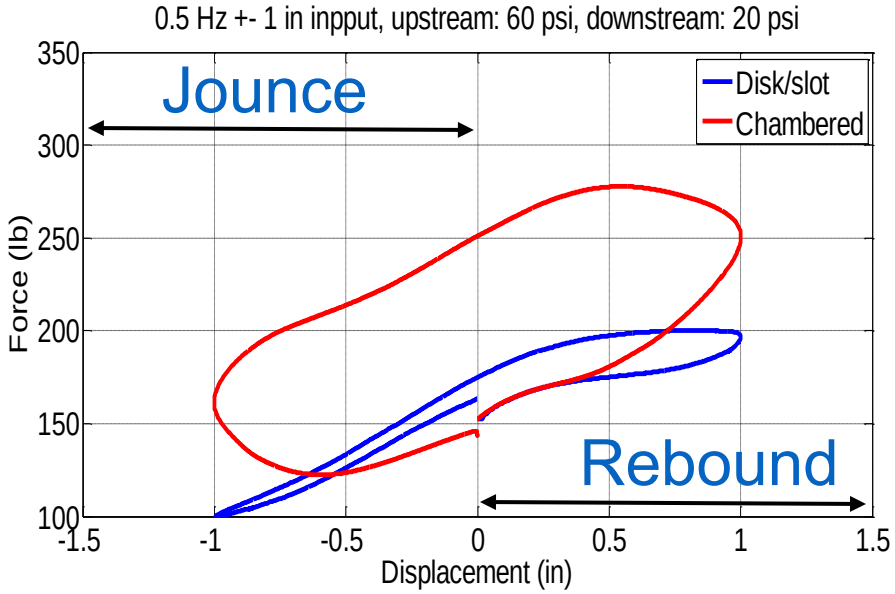

Figure 29. Force-displacement hysteresis plot of the airspring in line with both chambered and disk/slot valves under 0.5 Hz and +/- 1 in displacement input

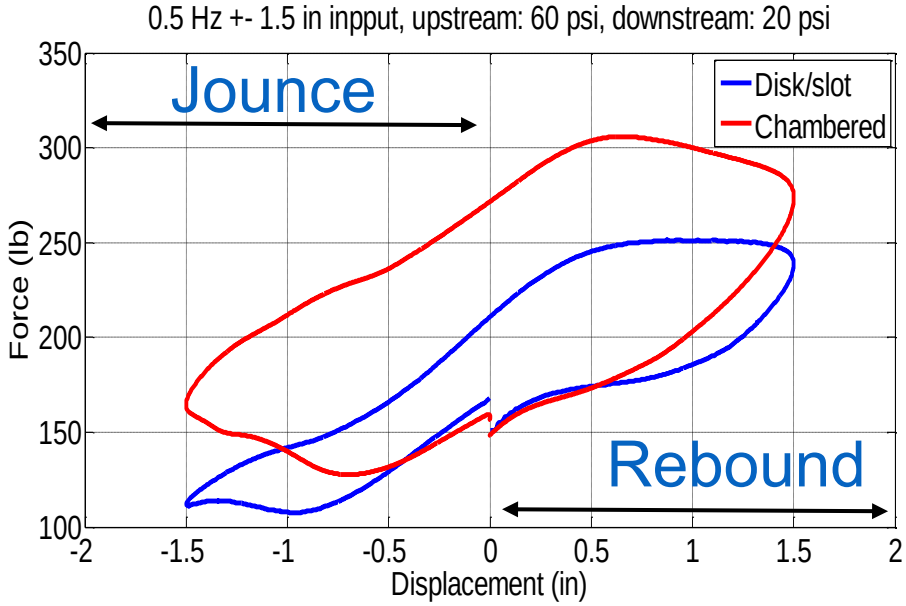

Figure 30. Force-displacement hysteresis plot of the airspring in line with both chambered and disk/slot valves under 0.5 Hz and +/- 1.5 in displacement input

By grouping the force-displacement hysteresis plot of the airspring, which is in line with both the disk/slot and chambered valves under the same frequency for three different input amplitudes (0.5 in, 1 in, and 1.5 in), higher force output can be seen with a larger amplitude input, as shown

in Figure 31 and Figure 32. The highest force value for the chambered valve is around 400lbs, but it is only 300lbs for the disk/slot valve. Also, it is interesting to see that the hysteresis loop for the disk/slot valve under 0.25 Hz and 0.5 in displacement input has virtually no enclosed area. This means that net energy input to the airspring is zero, hence, the air tank does not have the ability or time to charge any air into the airspring. A situation like this is unacceptable in reality. If a semi-truck and trailer has this type of valve installed, it will be more prone to roll-over with a disk/slot valve compared to the chambered valve. Additionally, it is clear that the purge flow rate of the chambered valve is higher because we can see a significant gap between the starting position and the ending position. Conversely, all hysteresis loops for the disk/slot valve have higher supply and purge rates.

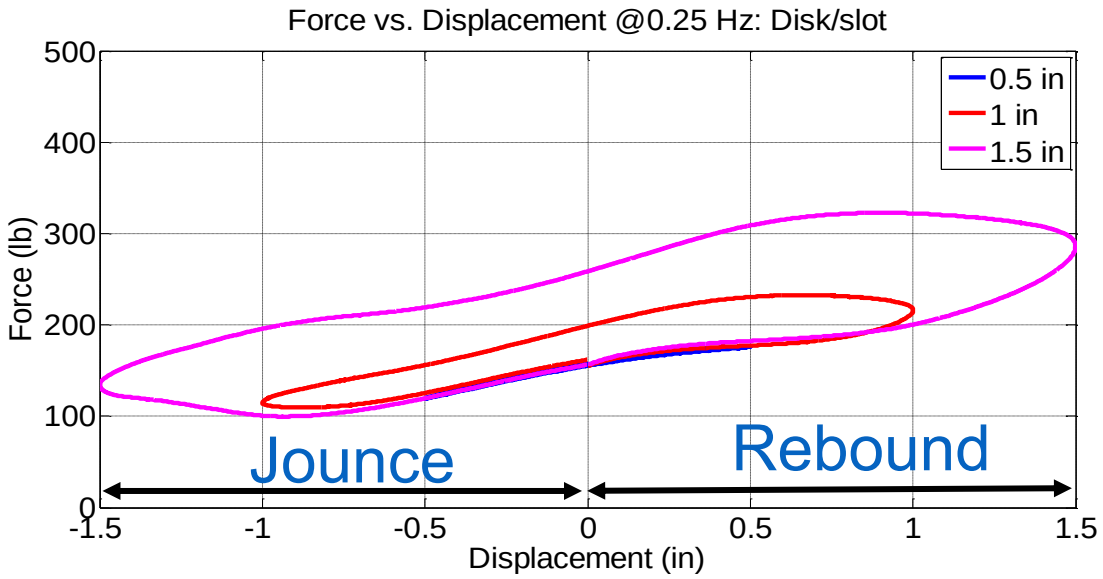

Figure 31. Force-displacement hysteresis plot of the airspring in line with the disk/slot valve under three different input amplitudes: 0.5 in, 1 in, and 1.5 in

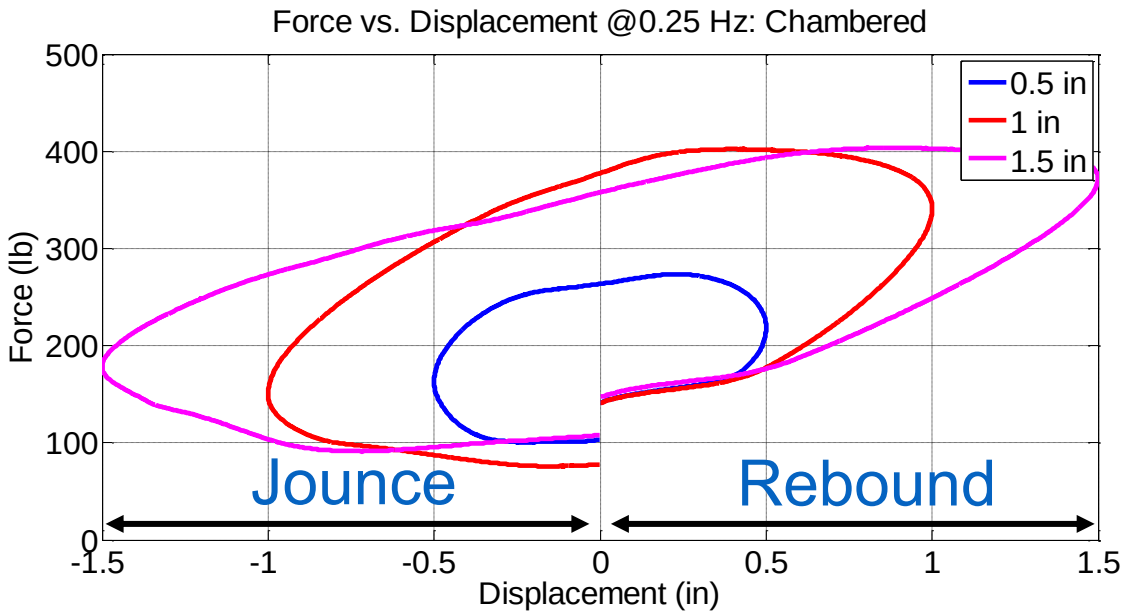

Figure 32. Force-displacement hysteresis plot of the airspring with the chambered valve under three different input amplitudes: 0.5 in, 1 in, and 1.5 in

Similarly, by grouping the force-displacement hysteresis plot of the airspring with both the disk/slot and chambered valves under the same amplitude, but for four different input frequencies (0.25 Hz, 0.5 Hz, 1 Hz, and 2 Hz), a higher force output can be seen for a smaller frequency input, as shown in Figure 33 and Figure 34. These figures show that hysteresis in a force-displacement cycle slowly decreases when the excitation signal frequency changes from 0.25 Hz to 2 Hz. The airspring consumes more energy in a quasi-equilibrium process (lower frequency [17]) than in a dynamic process (higher frequency). Nonetheless, the hysteresis in this experimental plot is overly affected by heat exchange due to indefinite estimation of polytropic coefficient. In reality, all pneumatic suspensions result in neither isothermal nor an adiabatic process. A polytropic process is a much better description for pneumatic suspensions, but in normal use, this process is much closer to adiabatic than isothermal [2]. Normally, when the excitation frequency is higher than 1 Hz, an adiabatic process can be assumed for the air inside the airspring. This indicates no heat exchange between the airspring and the ambient surroundings. Consequently, hysteresis is largely induced by material damping of the airspring rubber bellow [17].

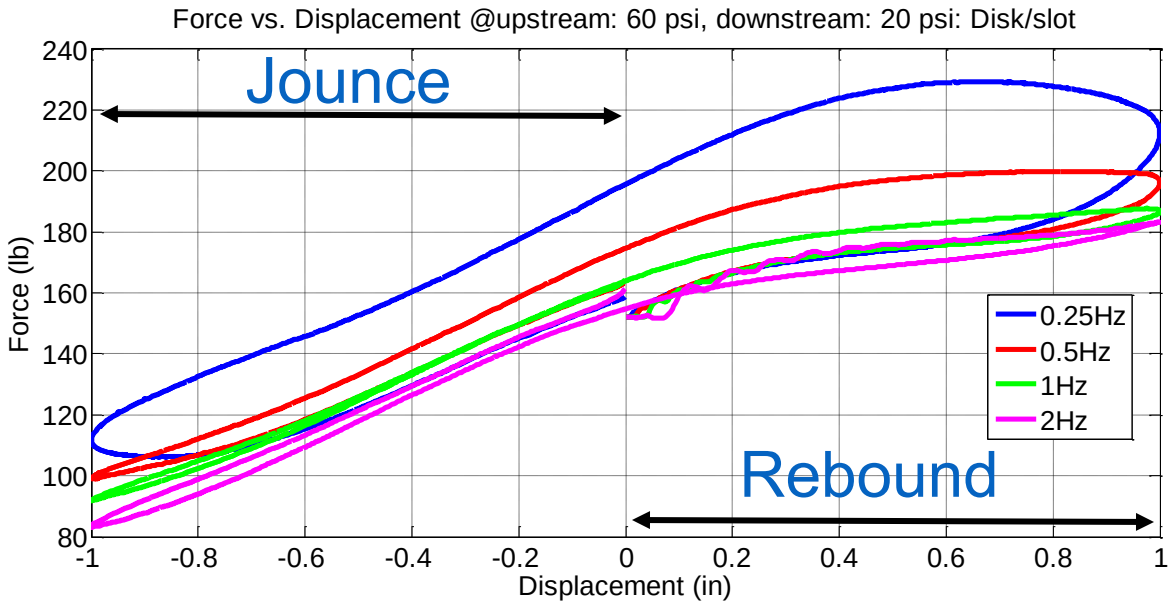

Figure 33. Force-displacement hysteresis plot of the airspring in line with the disk/slot valve under four different frequency inputs: 0.25 Hz, 0.5 Hz, 1 Hz, and 2 Hz

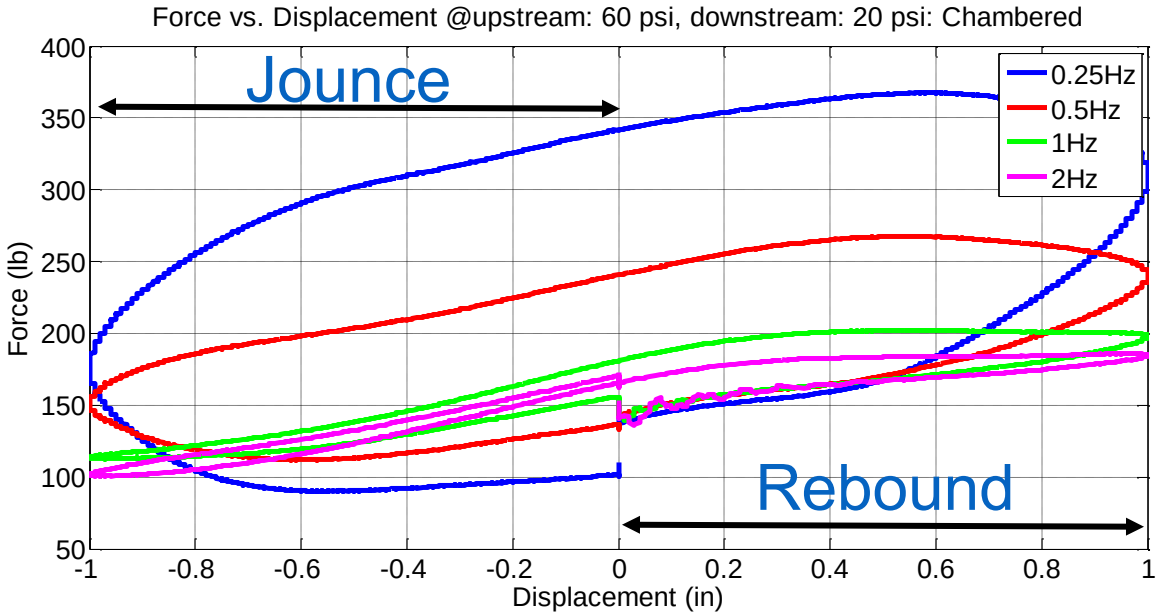

Figure 34. Force-displacement hysteresis plot of the airspring in line with the chambered valve under four different frequency inputs: 0.25 Hz, 0.5 Hz, 1 Hz, and 2 Hz

4. Flow Curve Reshaping and Redesign of the Disk/Slot Valve

4.1 Lever Arm Length Optimization

At this point, all the air flow characterization tests have successfully been completed, and the results verified with airspring tests. The air flow rate of the chambered valves is approximately four times higher than the disk/slot design in the transient region. In this region, air mass flow rate changes dramatically with little change in arm rotation angle. The goal is to redesign the disk/slot valve to make it comparable in this transient operation region without compromising the original structural integrity of the disk/slot valve assembly. The design concept follows "Everything should be made as simple as possible but not one bit simpler" by Albert Einstein. Logically, the first design change would be to the leveling arm because it is the least complicated part which wouldn't require any major change in the entire assembly. When arm length is involved in the picture, it is better to express deadband in terms of displacement instead of arm rotation angle. Moreover, if the leveling arm is cut to a relatively short length, small angle assumption is no longer valid. The leveling arm is then tested with 4 different lengths: 7.25 in, 6.25 in, 5.25 in, and 4.25 in. Eight displacement setpoints in inches (0.3, 0.6, 0.9, 1.2, 1.5, 1.8, 2.1, and 2.4) were used to accurately calibrate the relationship between arm angle of rotation and suspension travel. Angles of rotation were recorded using a Honeywell hall-effect rotary position sensor, and results are shown in Figure 36 . From previous chapters, we know that the deadband for the disk/slot valve is around +/- 2 degrees of arm rotation, and the deadband for the chambered valve is only about +/- 1.1 degrees of arm rotation. The values of deadbands in terms of arm angle of rotation will not change. For the chambered valve with a 7.25-inch leveling arm, the deadband was 0.132 in in terms of suspension travel. Similarly, the deadband of the disk/slot valve was determined to be 0.24 inch. Now, suspension travel of 0.132 in becomes a benchmark parameter, and it is used to find a minimum leveling arm length that would satisfy disk/slot deadband of +/- 2 degrees of rotation. It turns out that 3.625 in of leveling arm would satisfy this requirement. This newly-determined arm length would provide the same deadband (0.132 in) as the chambered valve.

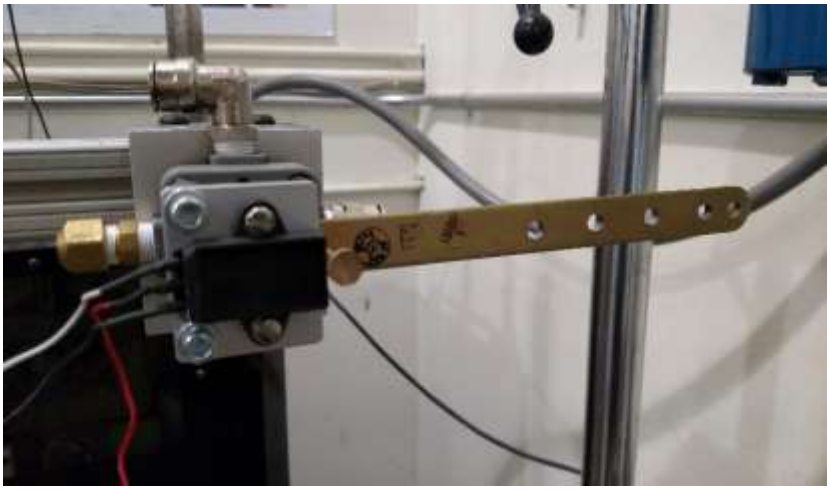

Figure 35. Arm rotation angle to suspension travel calibration experimental setup

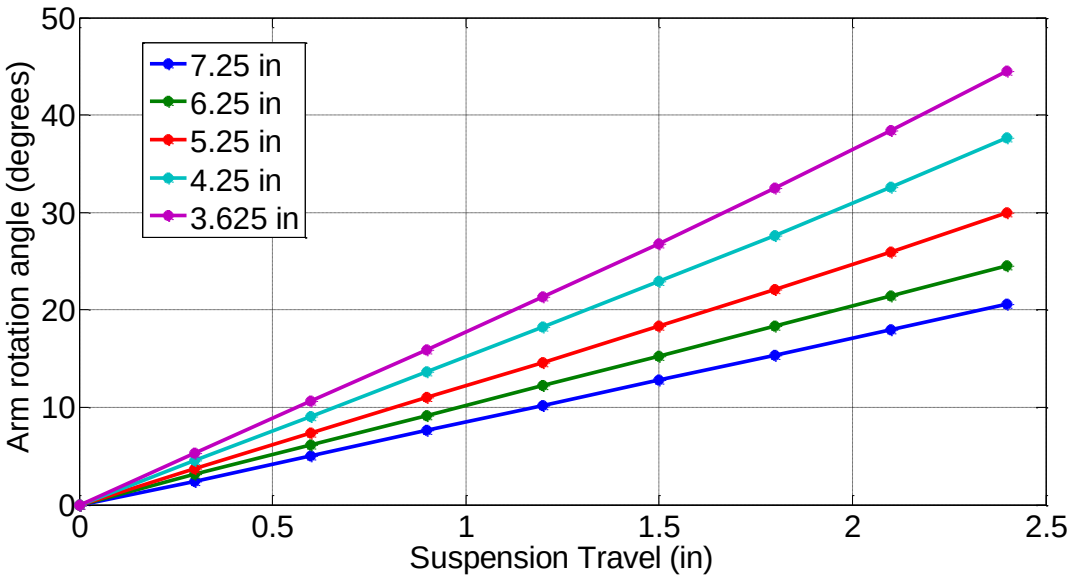

Figure 36. Arm rotation angle to suspension travel calibration curve

4.2 Flow Curve Reshape Theory and Design Consideration

Next, the disk/slot valve can be functionally considered to be an air path with variable area orifice. The air mass flow rate though an orifice is given as a function of upstream and downstream pressure and the effective area of the orifice, it is expressed as [32] and [19]:

$$\dot{m}_L = A \cdot C_f \cdot P_{up} \cdot \sqrt{\frac{2 \cdot n}{R \cdot T_{up} \cdot (n+1)}} \cdot \left(\frac{2}{n+1}\right)^{\frac{1}{n-1}} \quad \left[\frac{p_{dn}}{p_{up}} \leq \left(\frac{2}{n+1}\right)^{\frac{n}{n-1}}\right] \qquad \textit{Equation 7}$$

$$\dot{m}_L = A \cdot C_f \cdot P_{up} \cdot \sqrt{\frac{2 \cdot n}{R \cdot T_{up} \cdot (n-1)}} \cdot \sqrt{\left(\frac{P_{dn}}{P_{up}}\right)^{\frac{2}{n}} - \left(\frac{P_{dn}}{P_{up}}\right)^{\frac{n+1}{n}}} \quad \left[\frac{p_{dn}}{p_{up}} > \left(\frac{2}{n+1}\right)^{\frac{n}{n-1}}\right] \qquad \textit{Equation 8}$$

The following definitions apply:

$A = orifice\ area\ (in^2)$

$P_{up} = upstream\ pressure\ (psi)$

$P_{dn} = downstream\ pressure\ (psi)$

$C_f = flow\ coefficient$

$R = specific\ gas\ constant$

$n = polytropic\ exponent\ for\ air\ (approximately\ 1.4)$ [32]

$\left(\frac{2}{n+1}\right)^{\frac{n}{n-1}} = 0.53$

where C_f can be adjusted from the theoretical value to a value that is more suitable to this experiment. These adjustments include the losses resulting from friction, loss of kinetic energy, contraction/enlargement, and bends in the pipe. More importantly, we can conclude that the air mass flow rate is directly proportional to the valve orifice area. Also, the amount of orifice area is directly related to the rotation of the leveling arm that is caused by the vertical displacement of the driving axle with respect to the truck body and can be express by:

$$\begin{cases} A = 0 & |disp| < |deadband| \\ A = f(disp) & |deadband| \leq |disp| < disp_{\max flow} \\ A = A_{max} & disp_{\max flow} \leq |disp| \end{cases}$$

Therefore, the new orifice area should be four times larger than the original design, which means that the new orifice should be double in diameter of that of the original orifice.

4.3 CAD Parametric Studies

In order to have a more precise parametric study of the geometry, a CAD model of the two most critical parts of the disk/slot valve, disk and orifice, is needed. As shown in Figure 37, all the dimensions are measured using a digital caliper. Although it is extremely difficult to determine an exact measurement of the original disk geometry because the valve manufacturer did not provide us with one, it is deemed to be the most accurate measurement of geometry that can be made. Two straight edges can be seen at the two ends of the slot on the disk. The reason behind this design is that the straight edge allows more air to flow through the orifice compared to a rounded edge when it first starts to be uncovered by the rotary motion of the disk.

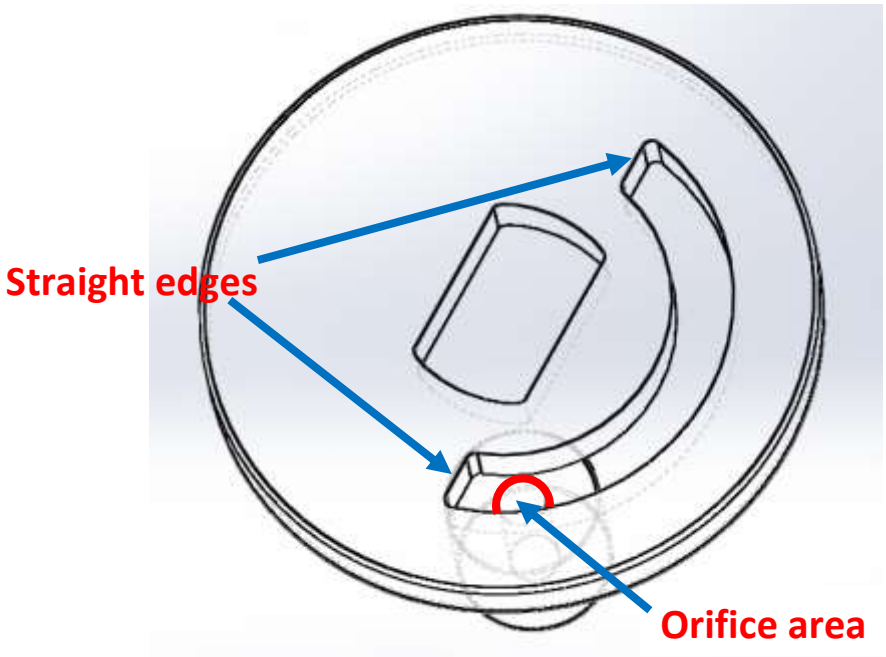

Figure 37. SolidWorks model of the disk/slot valve. Orifice is highlighted in red

To prove that a flat edge would give the valve a higher flow rate than the rounded edge, two equations which describe the behaviors of both cases are studied [33]. Firstly, a portion of a round disk whose upper boundary is a circular arc and whose lower boundary is a chord is shown in Figure 38 below:

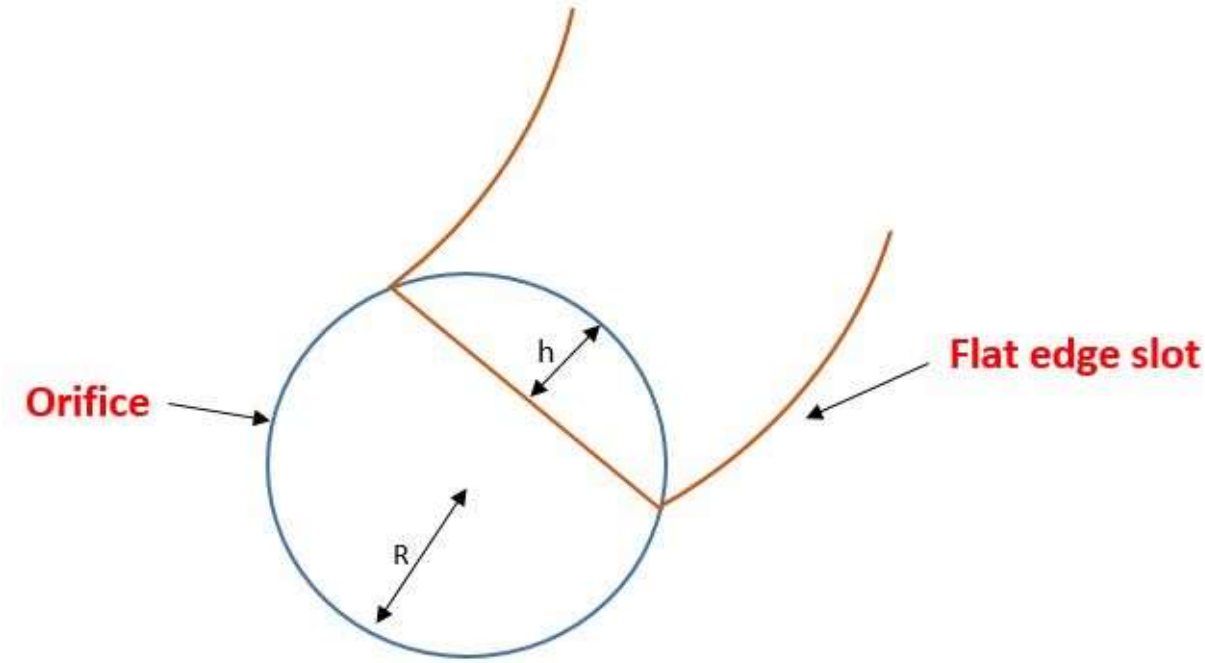

Figure 38. Illustration of the interaction between a flat edge slot and an orifice

The equation of this configuration can be expressed as [33]:

$$A = R^2\, cos^{-1}\left(\frac{R-h}{R}\right) - (R-h)\sqrt{2Rh-h^2} \qquad \textit{Equation 9}$$

where A is the cross-sectional area, R is the radius of the circle, and h is the width of the area that is uncovered, which is also equal to the product of angle of rotation of the disk and the disk radius. The angle of rotation of the disk can be expressed as:

$$\theta = \frac{Suspension\ travel}{Arm\ length} \qquad \textit{Equation 10}$$

Secondly, the interaction of two circles is studied and illustrated in Figure 39:

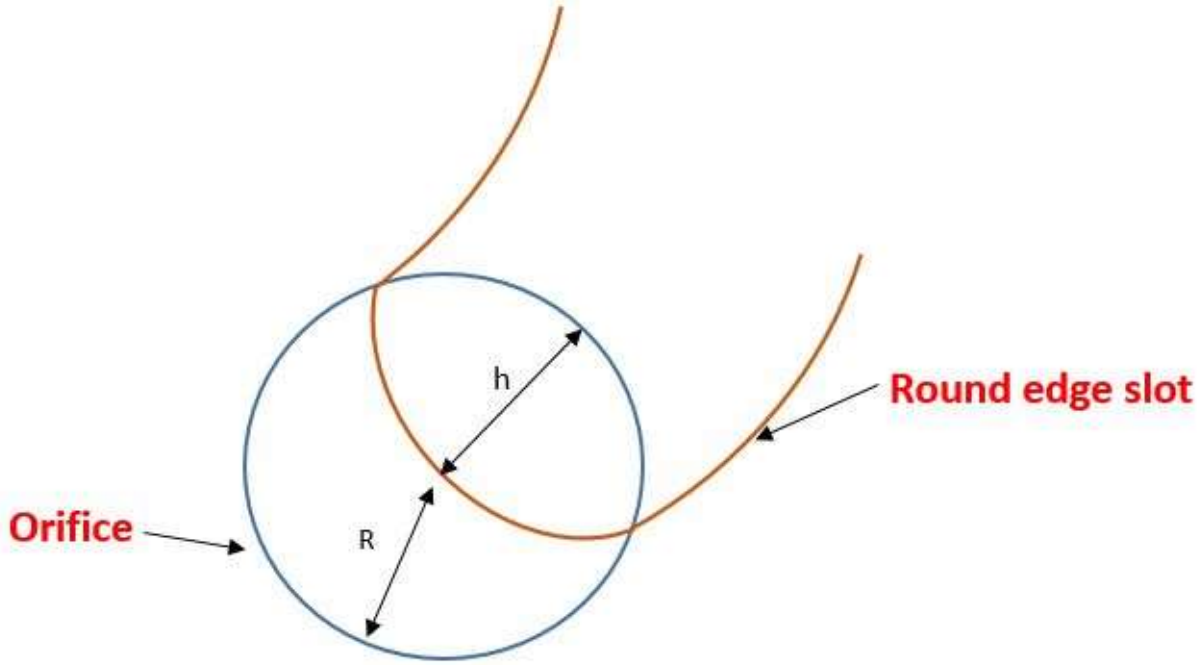

Figure 39. Illustration of the interaction between a round edge slot and an orifice

The equation of this configuration can be expressed as [33]:

$$A = r^2\,cos^{-1}\left(\frac{d^2+r^2-R^2}{2dr}\right) + R^2\,cos^{-1}\left(\frac{d^2+R^2-r^2}{2dR}\right) - \frac{1}{2}\sqrt{(-d+r+R)(d+r-R)(d-r+R)(d+r+R)} \qquad \text{Equation 11}$$

where r and R are the radii of both circles. If they are equal to each other, the above equation can be expressed as [33]:

$$A = 2R^2\,cos^{-1}\left(\frac{d}{2R}\right) - \frac{d}{2}\sqrt{4R^2-d^2} \qquad \text{Equation 12}$$

where d is the distance between the two centers of the two circles. A Matlab simulation of both scenarios is shown in Figure 40:

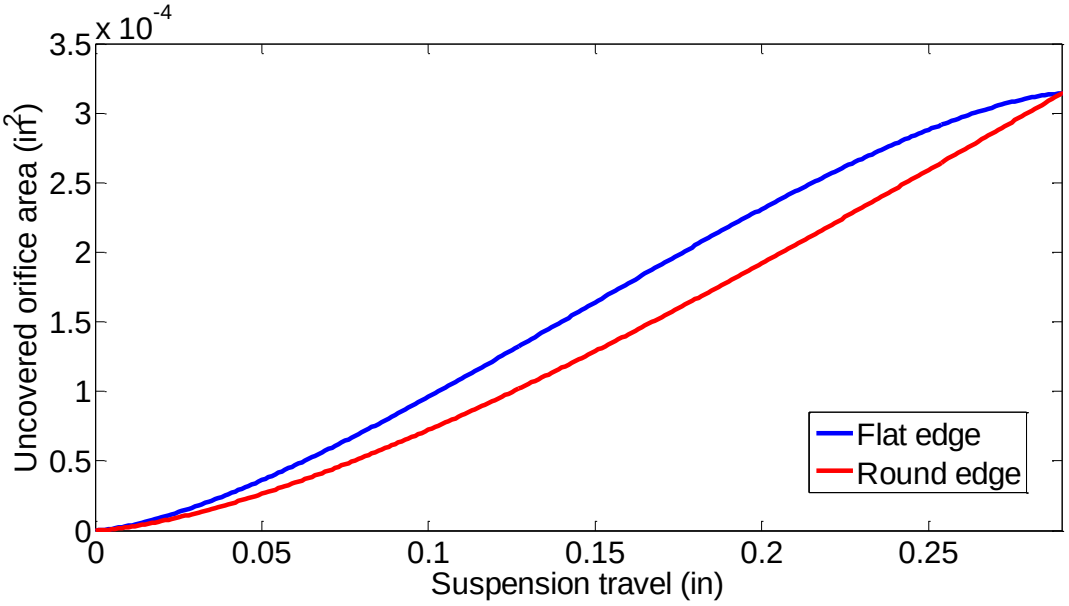

Figure 40. Matlab simulation of uncovered orifice area vs. suspension travel of both the flat edge and round edge slot

Realistic simulation parameters are used for this simulation. Lever arm length is set to 7.25 in, radius of the disk is set to 0.5 in, radius of the orifice is set to 0.1 in, and suspension travel is sweep from 0 to 1 inch in increments of 0.001 in. From Figure 40, it is clear that the flat edge design of the slot provides a larger uncovered orifice area compared to the round edge design throughout the entire range. The flat edge design is then incorporated into the new slot design due to its ability to provide a relatively larger flow rate. With this concept in mind, together with the idea of increasing the diameter of the orifice by double the original diameter (0.1 inch), a parametric study of the diameter of the orifice is performed in SolidWorks as shown in Figure 41. Indicated by Figure 42, the left-most dash line is marked as the beginning of the flat edge movement. The center dash line is constrained as the relative position between the center point of the orifice and the pivot point of the lever arm. The right-most dash line is the current position of the flat edge of the slot. When the orifice diameter is set to 0.1 in, the lever arm can only sweep around 14.5 degrees to reach the maximum cross-sectional area. However, the sweeping angle is able to increase to around 30 degrees of rotation when the diameter of the orifice is doubled.

Note that to achieve four times the larger orifice area, degree of rotation must be doubled. For instance, if the lever to rotates 10 degrees to have 0.1 in^2 of orifice area, it would need to rotate 20 degrees in order to achieve a 0.4 in^2 of orifice area. From the flow characterization curve of the disk/slot valve that I was developed in the previous chapter, a 16-degree and a 22-degree rotation for both supply and purge, respectively, are determined which would be able to provide four times the flow rate than the original design. The maximum areas for both supply and purge are 0.0176 in^2 and 0.025in^2 (0.149 in and 0.1784 in for diameters), though it is relatively difficult to implement such a design into the actual valve assembly. The difficulties encountered during machining of parts, the feasibility of implementing such a design, and reconsideration of the design will be discussed in a later section.

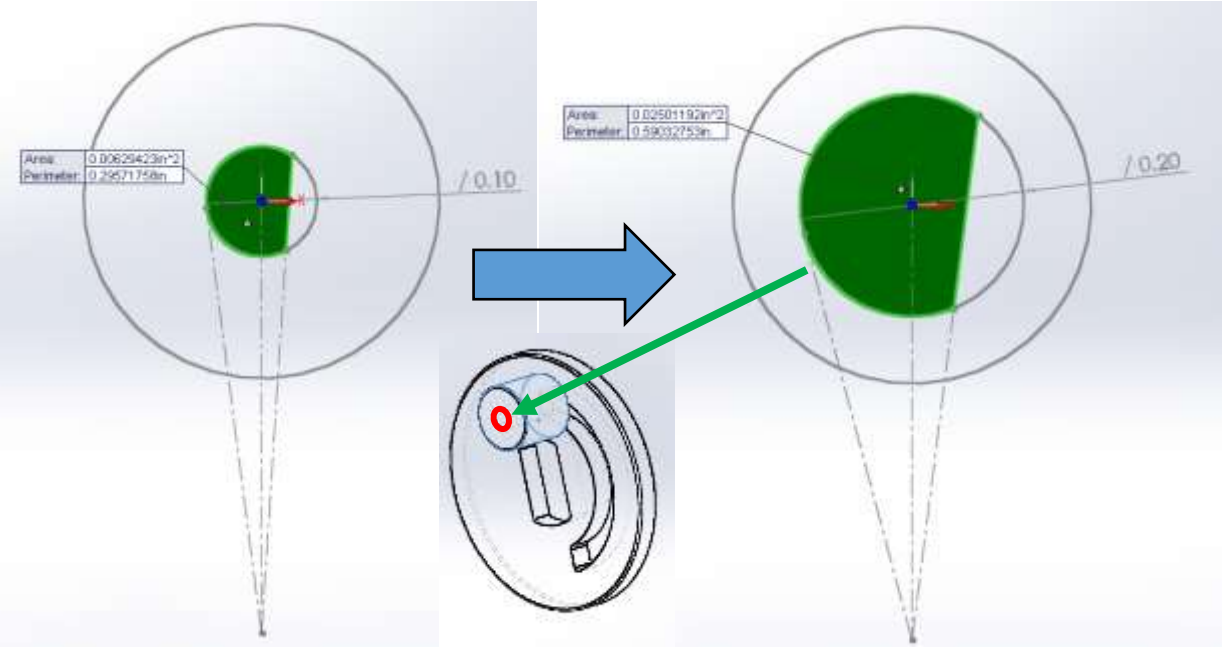

Figure 41. SolidWorks parametric study of the orifice area

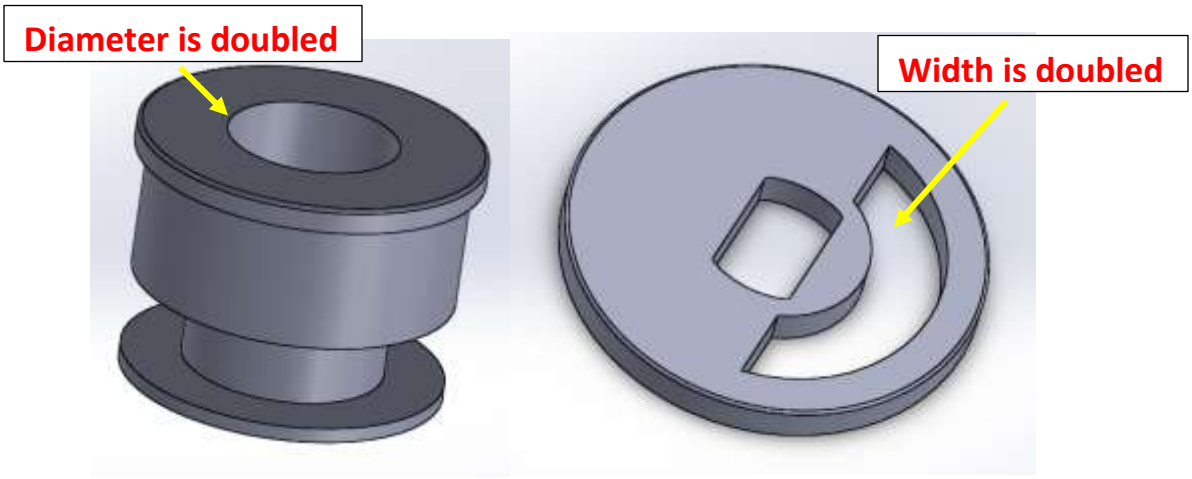

Figure 42. Redesigned bushing and disk from SolidWorks

4.3 Air Flow Predictions and Simulations

4.3.1 Air Flow Predictions

From the design that was discussed in the above section, a MATLAB simulation of the predicted flow curve, shown in Figure 43, can be generated using the same sets of parameters that were used to develop the original flow characterization curves. Flow rates match extremely well in the transient region, as shown by the bottom plot of Figure 43. The straight lines shown in the figure are caused by the cut-off maximum orifice area of the new design. The decision is made to limit the maximum flow area at suspension travels of 0.9 in and -1.3 in for both rebound and jounce, respectively, in order to have a reasonable maximum flow rate. An overwhelmingly large maximum flow rate is not necessarily a good objective. First of all, if the load-leveling valve is providing too much air into the airsprings, the truck and trailer may experience an undesirable jerk motion. This defeats the purpose of improving transient dynamics of heavy truck air suspensions. Second, the original aluminum housing of the disk/slot might not be able to tolerate such high air flow rates. The high air flow (especially purge) may distort the original structural integrity of the valve assembly. As for the exact amount of air flow that is most suitable for this

kind of valve or load-leveling valve in general, it is beyond the scope of this thesis. Further research can be done in order to answer that question.

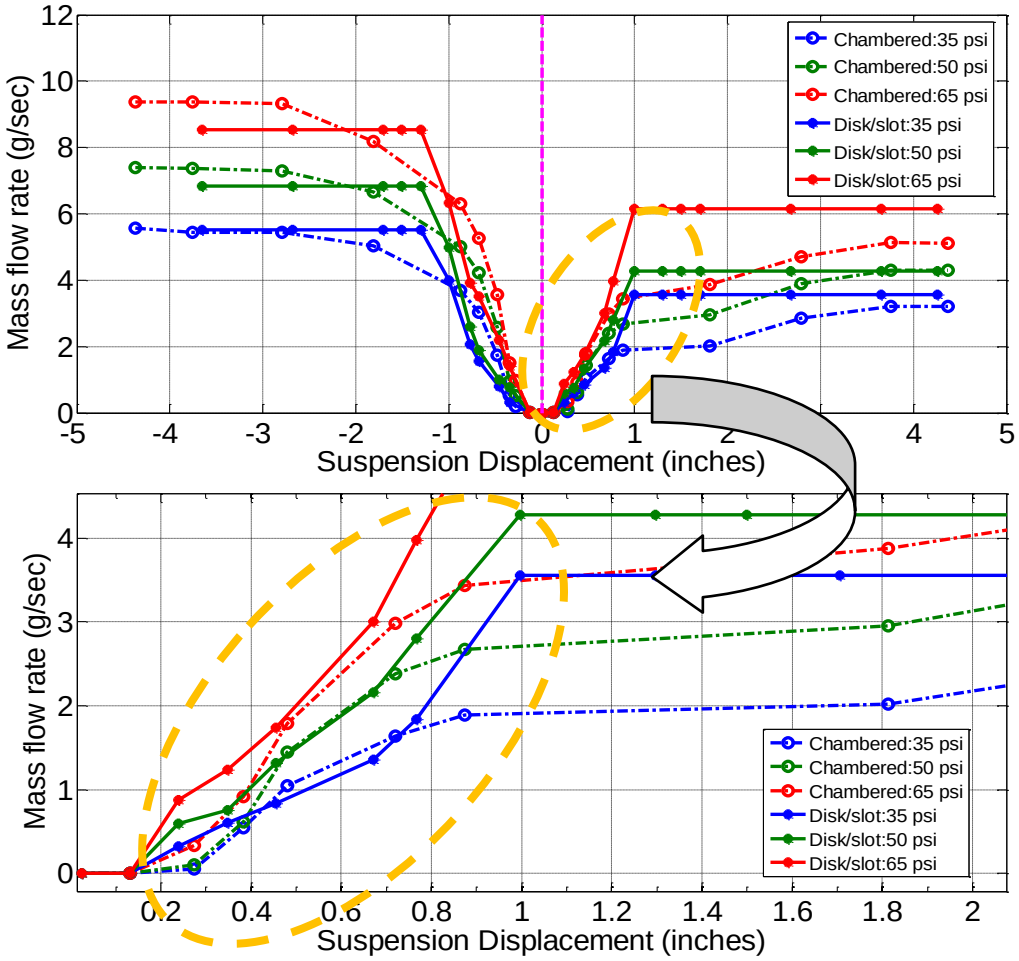

Figure 43. Matlab simulation of the predicted flow characterization curve. The top plot is the overview of both valves, and the bottom plot is a zoom-in view of just the transient part of the supply side

A cleaner plot of the predicted flow characterization curve under just 65 psi pressure difference between the upstream and downstream of the redesigned disk/slot valve is shown in Figure 44:

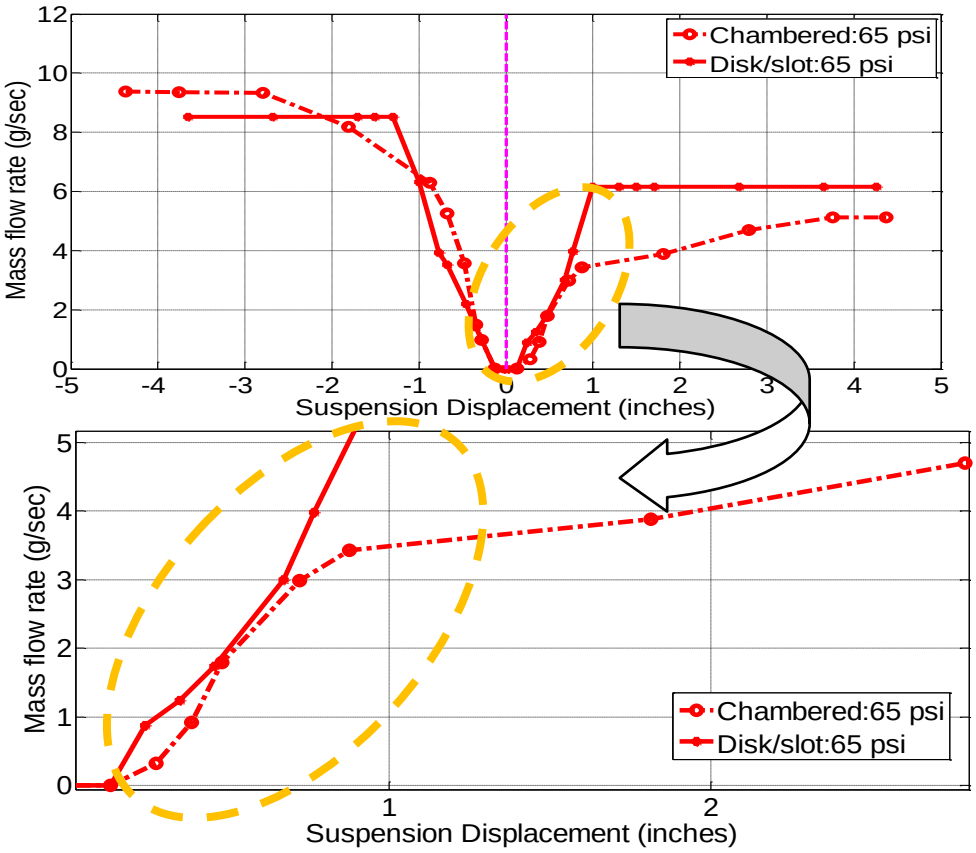

Figure 44. Matlab simulation of the predicted flow characterization curve of just the 65 psi pressure difference (most common case)

4.3.2 Simulation Results

As mentioned in the previous chapter, one of the most important functions that the flow characterization curve has is that it can be used as a critical input parameter to the modeling of the load-leveling valve, which is one of the most critical components of the heavy truck air suspensions. In order to have an accurate pneumatic suspension model, an experimentally developed characterization curve must be implemented into the overall consideration of the model. A simulation model of the pneumatic suspension system from the air tank to the airsprings is then developed by Chen, which also comprises the influence of all of the components used in the airsprings. Furthermore, dynamics of a multi-domain evaluation of a 9-degrees of freedom of the truck body (includes pitch, roll, and heave), and unsprung mass dynamics of the front and dual rear axles are included in this model [31]. This model is very

useful because of its ability to show how the air suspension affects the truck dynamics by changing some of the parameters of the pneumatic circuit. The pneumatic model that is implemented with the experimentally developed flow characterization curve is then coupled with a roll-plane model of the truck to evaluate the influence of the pneumatic suspension dynamics on the truck body roll, and determine how the forces are transmitted to the sprung mass [31]. Figure 45 shows the truck multibody dynamic model schematics with 9 degrees of freedom.

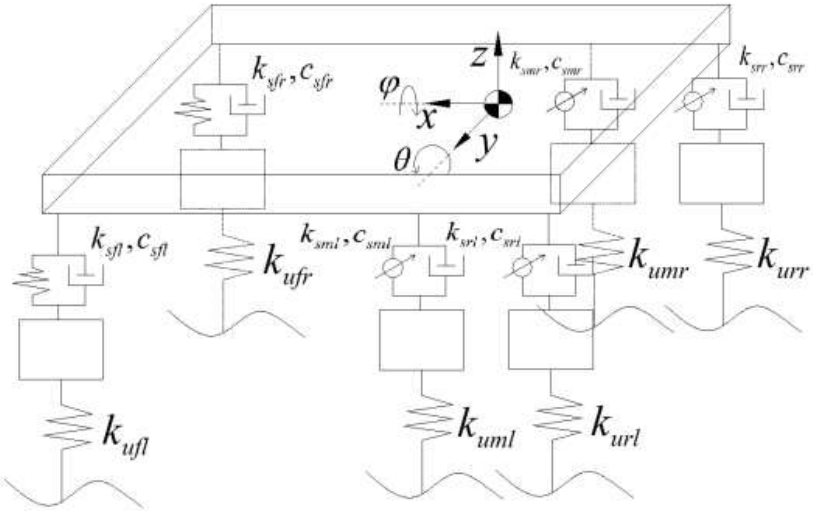

Figure 45. Truck multibody dynamic model schematics [31]

As shown in Figure 46, a lateral acceleration of 0.15 g over the span of 30 seconds is used as an input parameter to the dynamic truck model. The actual acceleration from 0 to 0.15 g happens in the first 3 seconds, and this is a realistic truck steady state cornering steering maneuver.

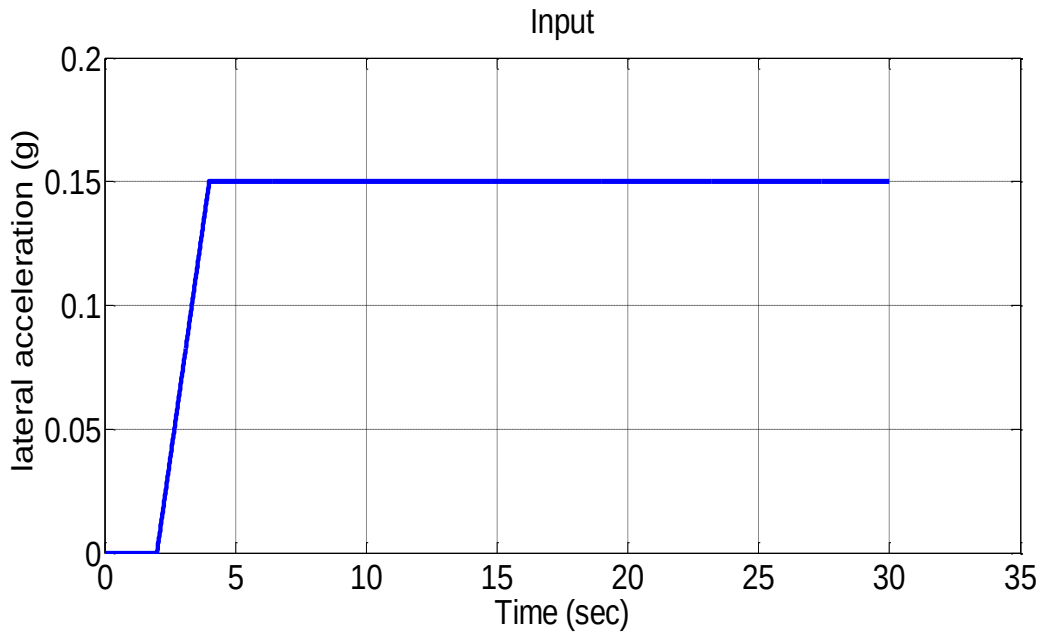

Figure 46. A lateral acceleration of 0.15 g is used as an input to the dynamic truck model

In the roll angle comparison plot of the chambered valve, the original disk/slot valve, and the improved disk/slot valve, we can clearly see that the truck experiences the least amount of body roll when coupled with the chambered valve, and it takes the least amount of time to straighten the truck body back to a comfortable position. On the contrary, the original disk/slot valve experiences the largest amount of body roll compared to the other two configurations. It also does not have the ability to straighten the truck back to a comfortable position in a competitive time period. After 30 seconds of constant lateral acceleration of 0.5 g, it still has a 1 degree body roll. The red line indicates the roll angle of using an improved disk/slot design valve. The improved valve has a similar behavior to that of the chambered valve. The roll angle difference is always within 0.1 degree, which is deemed to be a great improvement.

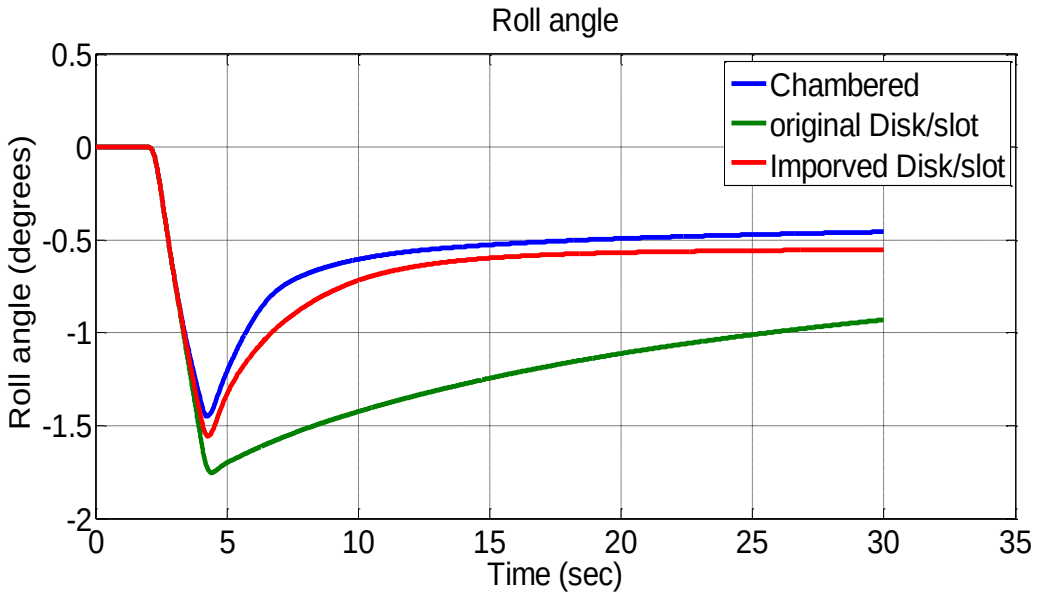

Figure 47. Roll angle comparison plot of the chambered valve, the original disk/slot valve, and the improved disk/slot valve

Figure 48 and Figure 49 show the simulated mass flow rate comparison of the right/left side chambered valve, the original disk/slot valve, and the improved disk/slot valve. From these plots, a huge difference between the mass flow rate through the valves between the original and the improved disk/slot valve design is shown. The original disk/slot valve only provides about 1.2 g/s of mass flow rate for the right side, and less than 1 g/s for the left side. However, both of the chambered and improved valves have almost 6 g/s mass flow rate for the right side and around 4 g/s mass flow rate for the left side. For the right side, the mass flow rate of the improved disk/slot valve even outperformed the chambered valve at its peak point. At this point, there is enough evidence that could prove the accuracy of the new design of the disk/slot valve. The next step would be to actually make a prototype of the new valve.

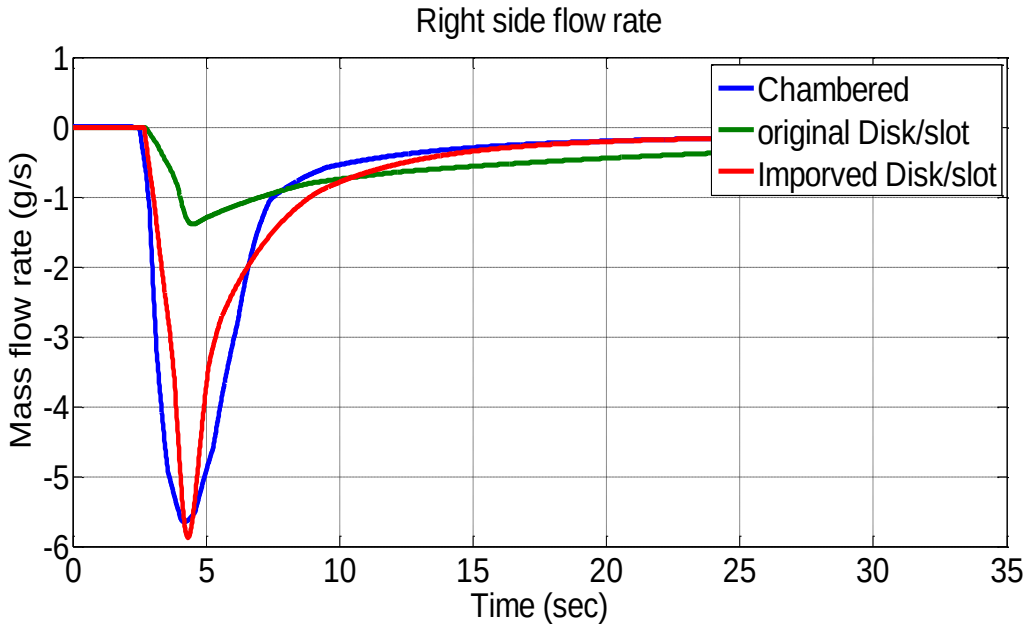

Figure 48. Simulated mass flow rate comparison plot of the right side chambered valve, the original disk/slot valve, and the improved disk/slot valve

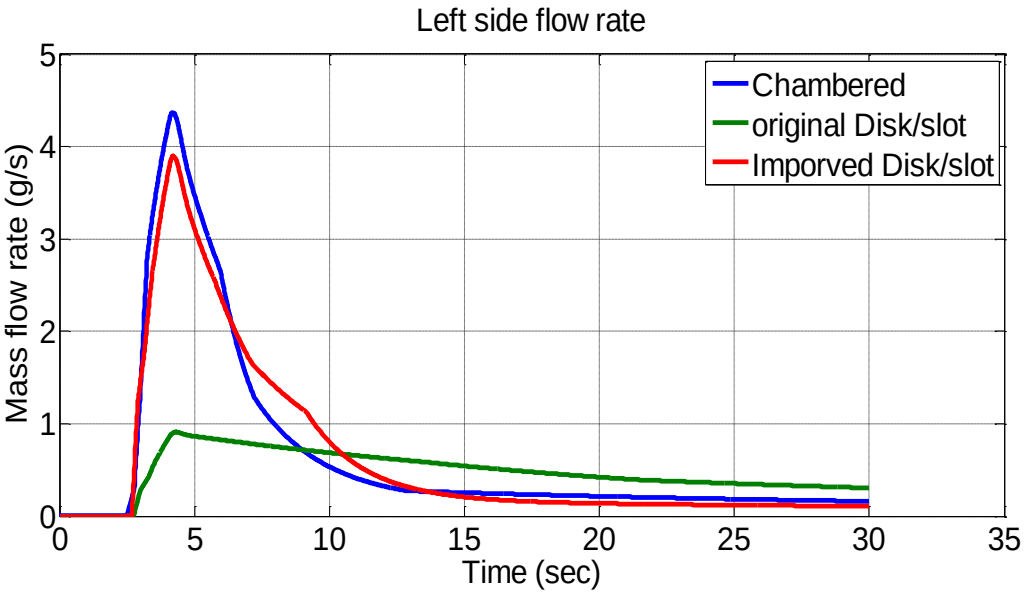

Figure 49. Simulated mass flow rate comparison plot of the left side chambered valve, the original disk/slot valve, and the improved disk/slot valve

4.4 Prototyping

In order to experimentally demonstrate the accuracy of the improved valve flow characterization predictions, a few new valve parts are precisely machined and polished. Six pieces of bushings with four times the orifice area of the original disk/slot valve and four pieces of disks with twice the slot width are cut using a water jet at Lynchburg Waterjet Cutting Inc. Note that the interaction surfaces between the disk and bushing are also polished to a near mirror-finish. These smooth interaction surfaces provide a tight seal with the help of grease. Larger retention springs and rubber O-rings are also purchased to better integrate into the new assembly. The rubber O-rings are used to create another lever of seal around the bushings. Similarly, the two straight holes which house the bushings are enlarged proportionally as well, as shown in Figure 50.

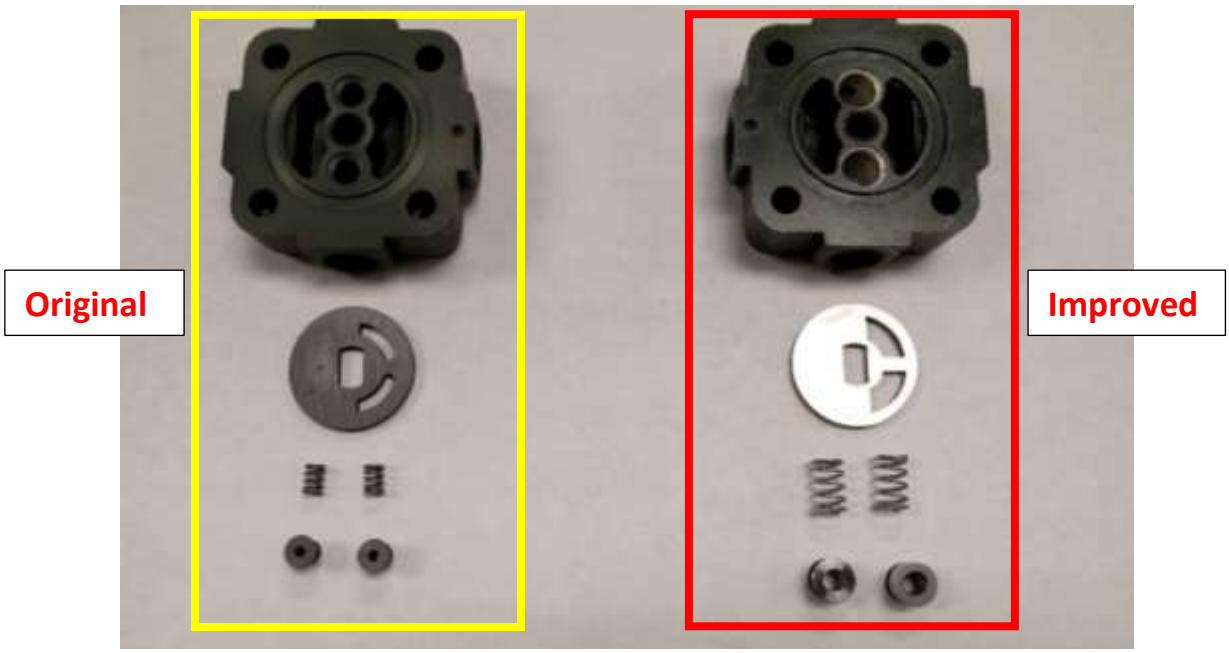

Figure 50. Side-by-side comparison of the original (left) and improved (right) disk/slot valve

As discussed in the CAD parametric study section, the maximum areas for both supply and purge are 0.0176 in^2 and 0.025in^2 (0.149 in and 0.1784 in for diameters), but the actual maximum orifice area is 0.04 in^2. It is difficult and costly to implement such a design into the actual valve assembly with a flat edge. This would introduce difficulties during machining of the parts.

Instead of cutting a flat edge of the orifice in the bushings, secondary orifices on the valve casing ports are found and drilled to match the areas of the corresponding requirements.

Last but not the least, as shown in Figure 51, the flat edge of the improved disk is slightly shifted to the right by $0.05\ in$ in order to preserve the same deadband (in terms of lever arm rotation angle) that the original disk/slot valve had. Because the diameter of the orifice of the bushing is doubled from $0.1\ \ in\ to\ 0.2\ in$. This small detail is especially important because the improved valve might be extremely sensitive and prone to any tiny road noise if the offset is not properly considered.

Figure 51. Two disks are stacked on top of each other (original disk is on top). The flat edge of the improved disk is slightly shifted to the right in order to preserve the same deadband

As shown in Figure 52, the newly-machined parts fit particularly well inside the original casing of the disk/slot valve. The walls around the two bushing holes have plenty of material left to support the pressure coming from both the high pressure air flow and tight fittings. The large O-rings sit on the bottom part of the casing and provide a third-layer seal. This satisfied the initial goal of enlarging the orifice area of the disk/slot design without compromising the structural integrity of the valve assembly.

Figure 52. The entire assembly of the improved disk/slot valve

4.5 Flow Characterization of the Newly Developed Valve

4.5.1 New Flow Curves

Referring to Chapter 3, Equation 6 is used again here so that the mass flow rate is dependent on the rate of change and instantaneous upstream pressure of the load-leveling valve. A schematic of the flow characterization system is presented in Figure 17. This test setup is valid because it has a constant pressure side and a variable pressure side. To test the supply air flow, the supply port is connected to the air tank, and the to-airspring port is exposed to the atmosphere. An upward lever movement would introduce a pressure drop on the upstream side of the load-leveling valve which is captured by the pressure transducer. In opposition, the air tank can also be connected to the out-to-air spring port when measuring the purge air mass flow rate. A downward motion of the lever arm would lead to a pressure drops on the upstream side. Pressure drop at various arm rotation angles were tested in Chapter 3. Figure 53 shows the new flow curves of the improved disk/slot valve plotted against the chambered valve. Clearly, a much improved flow rate can be seen across the entire input displacement range. A close look at the transient portion of the flow characterization curves shows a good match between the chambered

valve and the improved disk/slot valve in *Figure 54*. This portion is the most critical part of the truck suspension movement as was discussed in the previous chapter. The goal of reshaping the original disk/slot valve to match the chambered valve is achieved through precise metering, calculation, machining, and instrumentation.

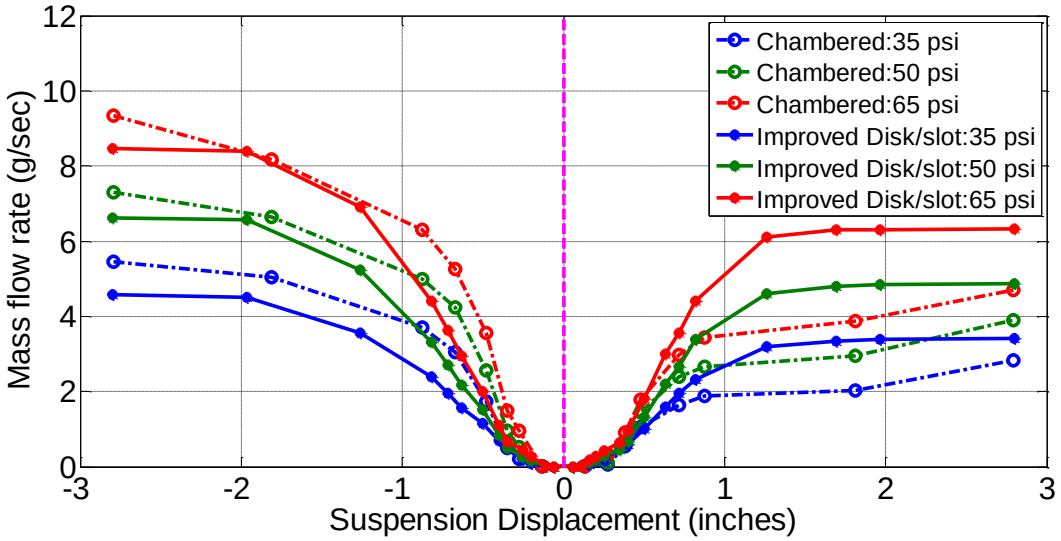

Figure 53. Flow characterization curves of the chambered valve and the improved disk/slot valve

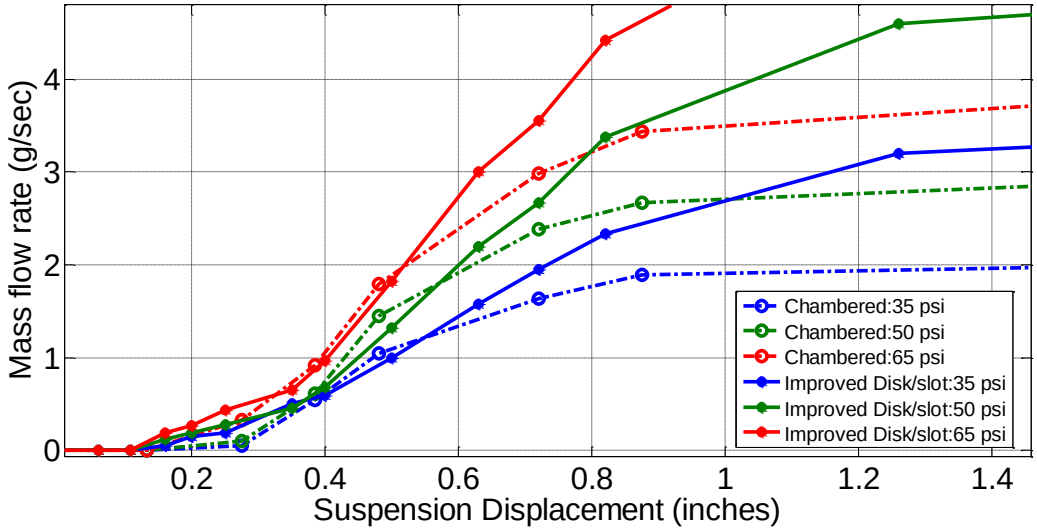

Figure 54. A close look at the transient portion of the flow characterization curves shows a good match between the chambered valve and the improved disk/slot valve

Figure 55 and Figure 56 proved that the prediction of air flow of the newly-designed valve was accurate. The zoomed-in view of the transient portion of the flow characterization curves revealed that my prediction is usually within +/- 0.2 g/sec in terms of air mass flow rate. This level of accuracy is highly desirable and is the best that could be achieved given the complexity of the experiments. With the available dimensional tolerances in manufacturing processes, and the uncertainties of the instrumentations and experimental setups, this level of error is inevitable. Figure 57 bears a close resemblance to Figure 24 in terms of the overall curve shapes and the amount of mass flow rate. The only difference is that the solid lines in Figure 57 represent the improved flow characteristics rather than the characteristics of the chambered valve.

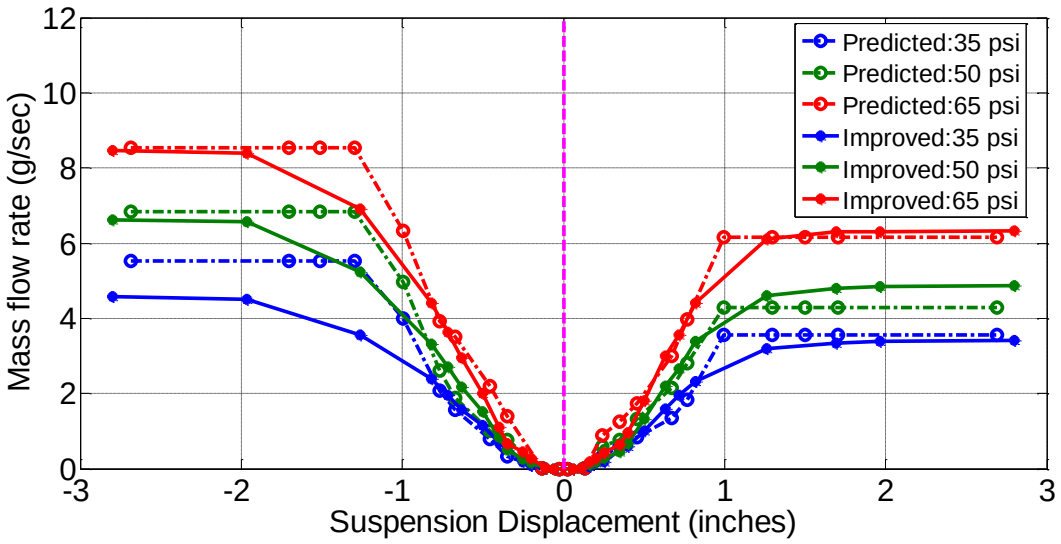

Figure 55. Flow curves of both the predicted and actual improved disk/slot valve

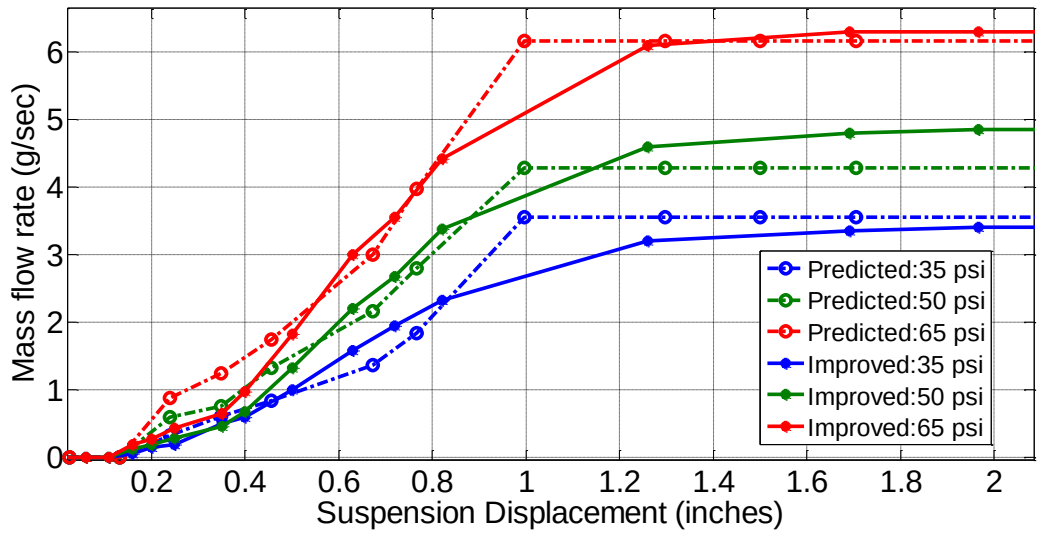

Figure 56. A close look at the transient portion of the flow characterization curve indicates a good agreement between the predicted and the actual results

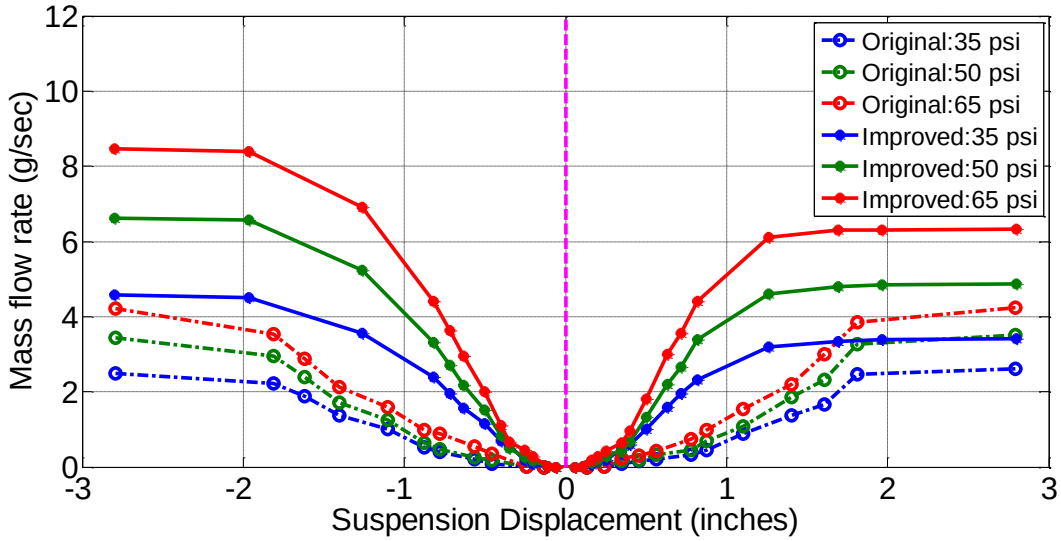

Figure 57. Flow characterization curves of the original and the improved disk/slot valve

4.5.2 Dynamic Airspring Verification Testing for the New Valve

Similar to the previous dynamic airspring verification tests, in order to validate the results of the newly-conducted flow characterization experiments and have a direct visual comparison of the valve performances on the airsprings, a verification process is needed. Six sets of experiments are conducted using two different sinusoidal input displacement frequencies of 0.25 Hz, and 0.5 Hz, coupled with three different amplitudes of 0.5 in, 1 in, and 1.5 in. The reason that both the 1 Hz and 2 Hz experiments were eliminated is that the valve does not supply or purge any air with these frequencies, as observed from Figure 33 and Figure 34. The small area inside the hysteresis curve is likely due to the effect of the airspring volume and cross-sectional changes. Therefore, there is no need to conduct such experiments which are likely to provide irrelevant results. All possible combinations are conducted with the purpose of simulating the actual semi-truck suspension deflections. An upstream pressure of 60 psi and a downstream pressure of 20 psi are set to have a 40 psi pressure differential. When the input displacement changes, dynamic stiffness of the airspring also changes. Figure 58 and Figure 59 clearly show a good match between the newly improved valve and the chambered valve. All the assumptions and the reasoning behind the discrepancies between the shapes of the hysteresis are explained in Chapter 3, Section 5. Also, air purge rate is much higher than the supply rate for the chambered valve and the improved valve. This is what causes the end point force value of the chambered valve to be lower than the starting position. As represented from Figure 58 and Figure 59, the chambered valve's hysteresis loops are very close to the improved valve, in both the shape and the resultant force value. Of course, they cannot be exactly the same, as has been discussed in the section above. This small error can be tolerated since the objective is to spot the overall trend/shapes of the hysteresis in order to verify the results from the new flow characterization experiments and validate the predictions.

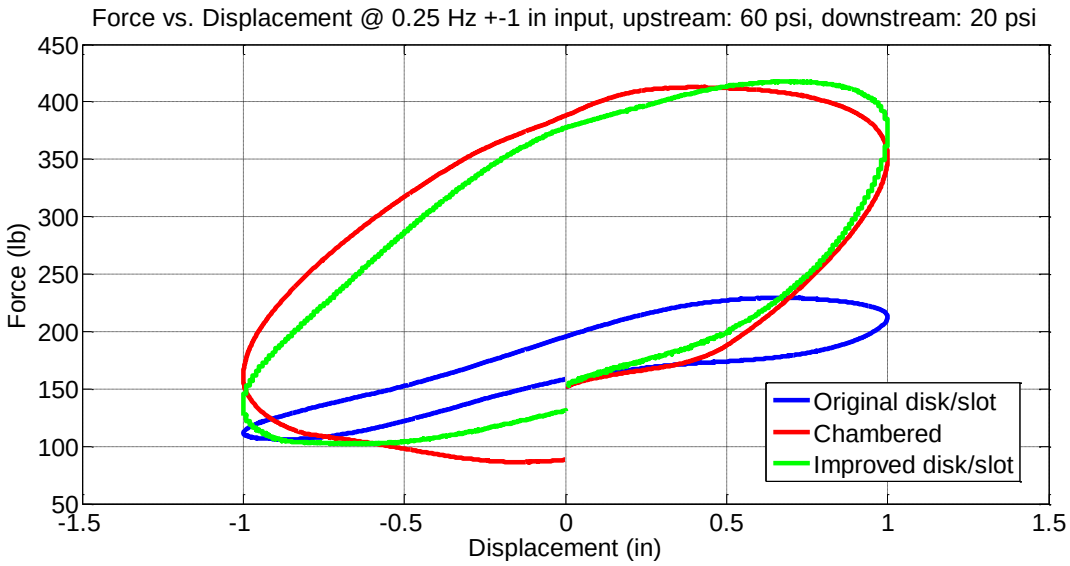

Figure 58. Force vs. displacement plot of 0.25Hz and +/- 1 inch displacement input with an upstream pressure of 60psi and downstream pressure of 20psi of the chambered, original, and the improved disk/slot valve

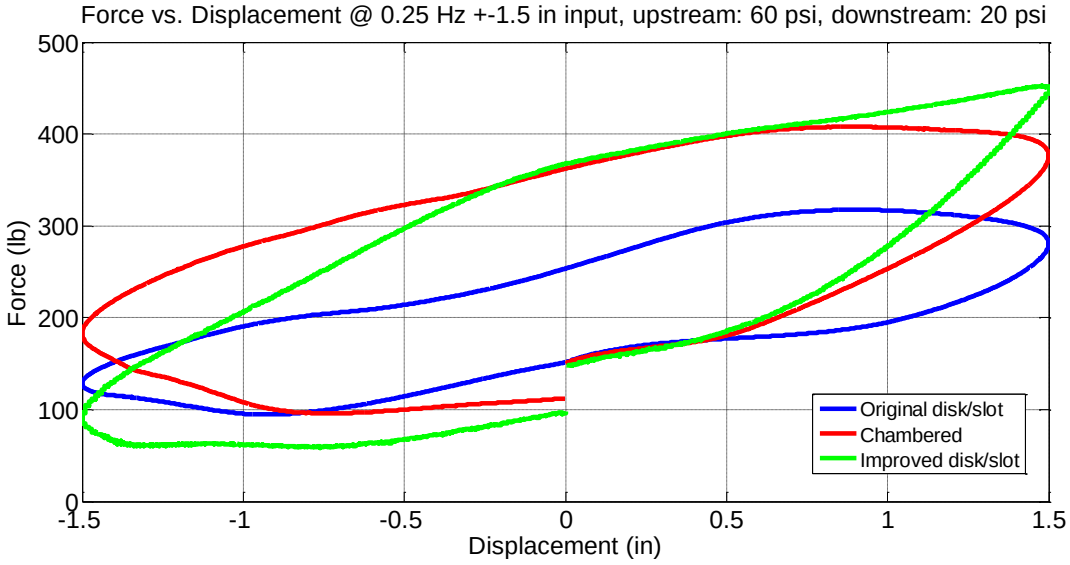

Figure 59. Force vs. displacement plot of 0.25Hz and +/- 1.5 inch displacement input with an upstream pressure of 60psi and downstream pressure of 20psi of the chambered, original, and the improved disk/slot valve

5. Concept, Summary and Conclusions

5.1 Independent Dual Motor-Valve Truck Air Suspension Testing Concept

Due to high cost, complexity, and time constraints, an alternative valve-testing concept is used that would allow for analysis of the roll dynamics of the truck without driving the truck on actual road. The idea behind this is that we can actually take the load-leveling valves out of the truck frame, and mount them on an externally built testing rig. As long as the valve body is fixed against a stable structure, the location of the placement of the valve does not matter. A precise rotation movement of the load-leveling valve arm can be controlled by two servo motors and an Adruino UNO microcontroller board combination, as shown in Figure 60 and Figure 61:

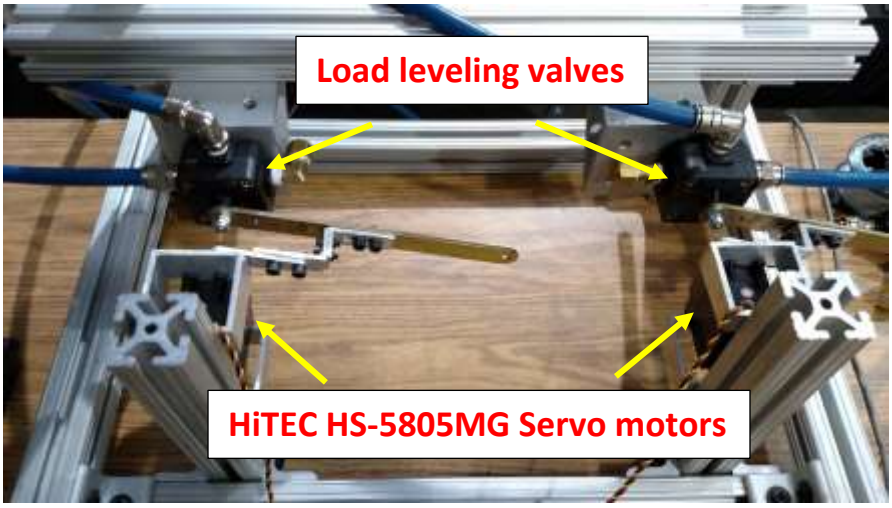

Figure 60. The testing rig for mounting both load-leveling valves and servo motors

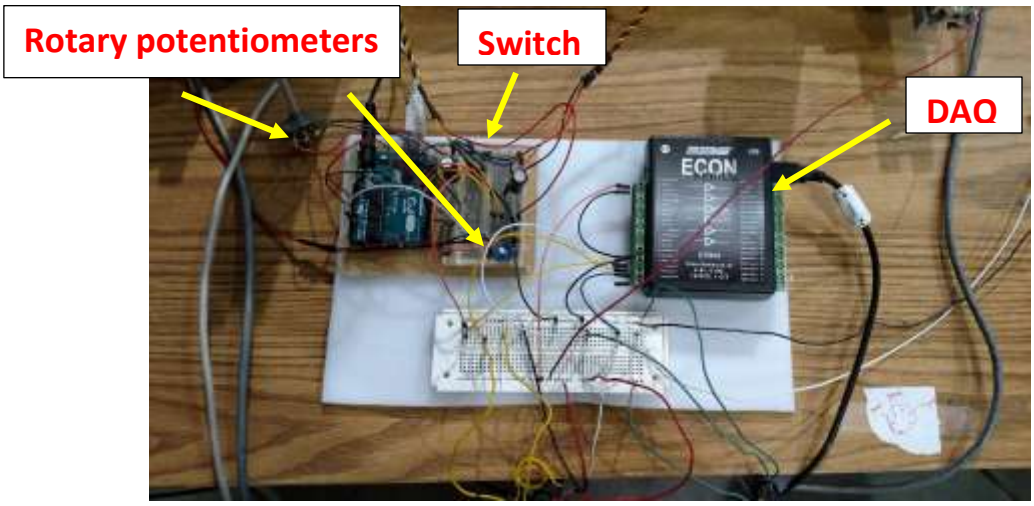

Figure 61. Adruino uno microcontroller is used to control the servo motors and Data Translation DT9816 DAQ module is used to record necessary information from all the sensors as well as the arm rotation motion

Two giant-scale HiTEC HS-5805MG servo motors are selected due to their high torque capability ($342oz \cdot in$) with a 6V power supply. The torque that is required to rotate the chambered valve with all the steel mounting brackets is determined to be around $1.2lb \cdot ft$, which is within the range of the selected motor's torque specifications. The rotational speed for the motor is 0.14 sec/60˚ which is also beyond the need of this testing. Two rotary potentiometers are used to independently adjust the initial lever arm position as shown in Figure 61; this data can also be utilized to calculate the roll angle with the measurements of geometry of the truck. As mentioned in previous chapters, initial neutral position is vital to all of these experiments. Therefore, being able to use the rotary potentiometer to fine-tune arm rotation angle and keep it within a reasonable range of the exact 0 degree angle is an absolute necessity. Moreover, the ability to freely adjust the lever arm position enables the possibility of tilting the truck to initial testing position. A switch is used to send a trigger signal to the controller, which has the ability to direct the motor to start or stop running the program that was coded in C language. The onboard Adruino 5V voltage supply was not enough to run both motors simultaneously with the chambered valves attached. Therefore, this voltage supply is then used to provide power to send command signals to the motors. An external 6V power supply is used to provide the power that is needed for the motors. One $2200\mu F$ capacitor is used to stabilize the unwanted wobble motion that is observed from the left motor. A pull-down resistor is used to hold the logic signal close to 0V when no other active device is connected. Figure 62 shows a

sample assembly of the chambered valve and Figure 63 shows that two string pots are used to measure the left and right side suspension deflections.

Figure 62. Sample assembly of the chambered valve

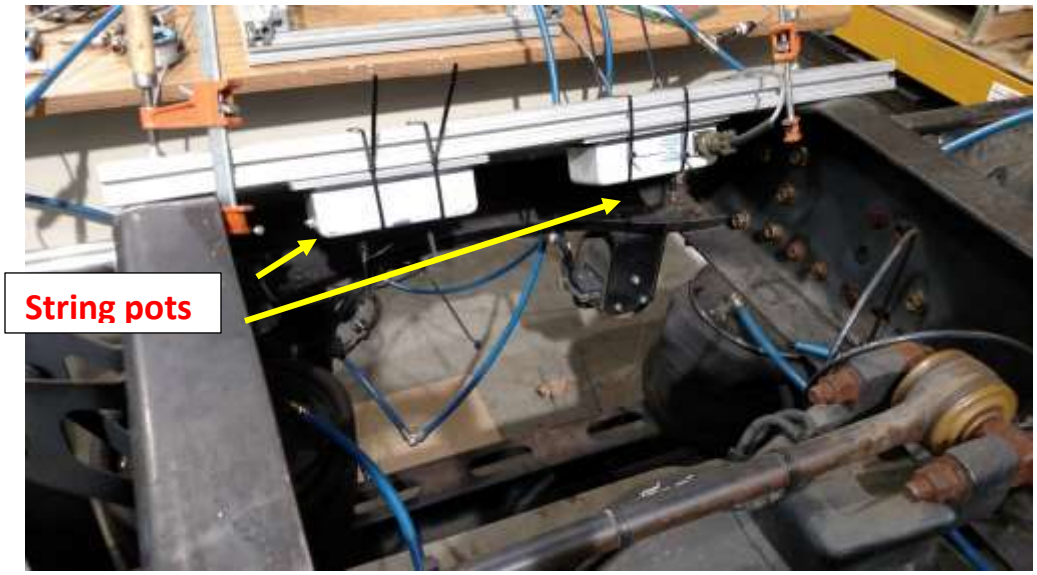

Figure 63. Two string pots are used to measure the left and right side suspension deflections

Also, two calibrated Honeywell pressure sensors are connected in line with both the left and right sides of the airsprings in order to measure the changing pressure inside the airsprings. All of this data is collected and recorded through Data Translation DT9816 DAQ module. A Matlab script

is also created to post-process the data. The entire setup is shown in Figure 64. This way, motion of the truck body can be easily controlled.

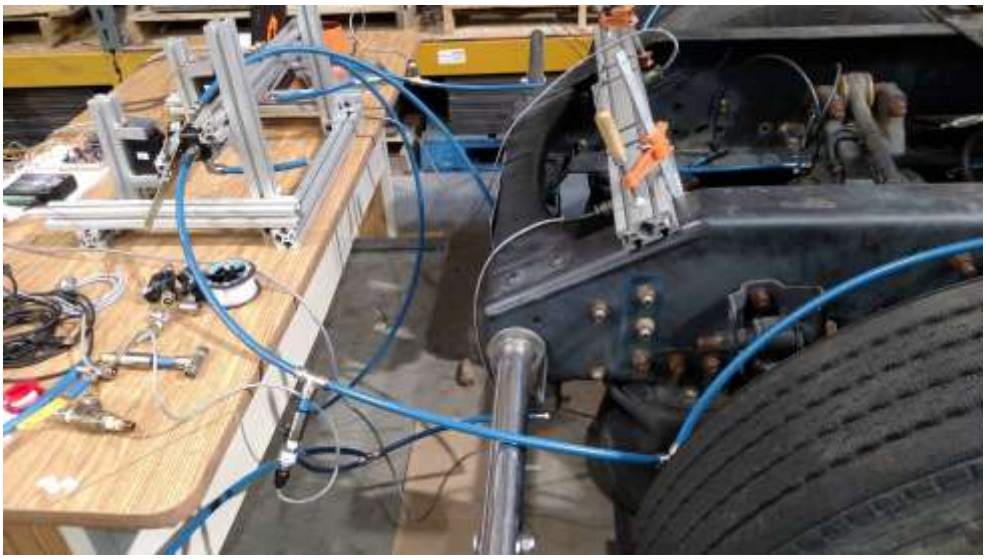

Figure 64. Entire setup of the independent dual motor-valve truck air suspension testing concept

The first set of experiments uses an input of 0.2Hz sinusoidal (180˚ out of phase) wave with 20 degrees of lever arm rotation amplitude. The sample result is shown in Figure 65 and Figure 66, and it is clear that the left side lever arm rotates up and the right side lever arm rotates down first because the left side hysteresis goes up first and vice versa. Note that none of these loops are able to perfectly close themselves because there is hardly any load on the truck, and it is extremely difficult to achieve the exact same amount of pressure inside both sides of the airsprings. As shown in Figure 65, the initial pressure of the left side airsprings is set to 12.5 psi, and the pressure of the right side airsprings is set to 12.3 psi. This small difference would make a huge impact on the outcome of the experiment. Notice that the dynamic stiffness of the left side airsprings is greater than the right side during the first quarter of this sinusoidal motion. This is due to the fact that the supply side (left) of the truck has a tiny initial pressure advantage at first, and this non-noticeable difference makes the entire truck frame go up even when both sides of the valves are doing the exact opposite arm motion. At this point, it was determined that this configuration cannot really represent the real truck dynamic system. In real life conditions, when truck airsprings actively experience a rebound motion (compression), the valves can passively provide air supply to the corresponding side of the truck. But in this setup, the valves are always

actively controlling the airsprings and providing a passive jounce motion. In order to accurately simulate realistic truck dynamics, an active truck frame motion input needs to be obtained through a more advanced setup which is beyond the scope of this thesis.

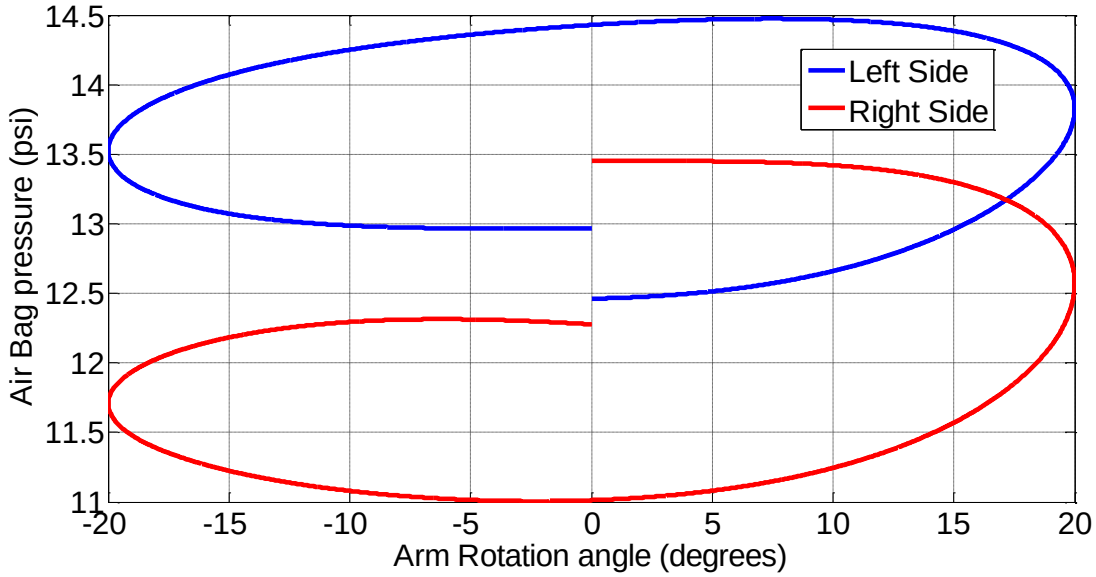

Figure 65. Sample airspring pressure plots of both right and left hand sides

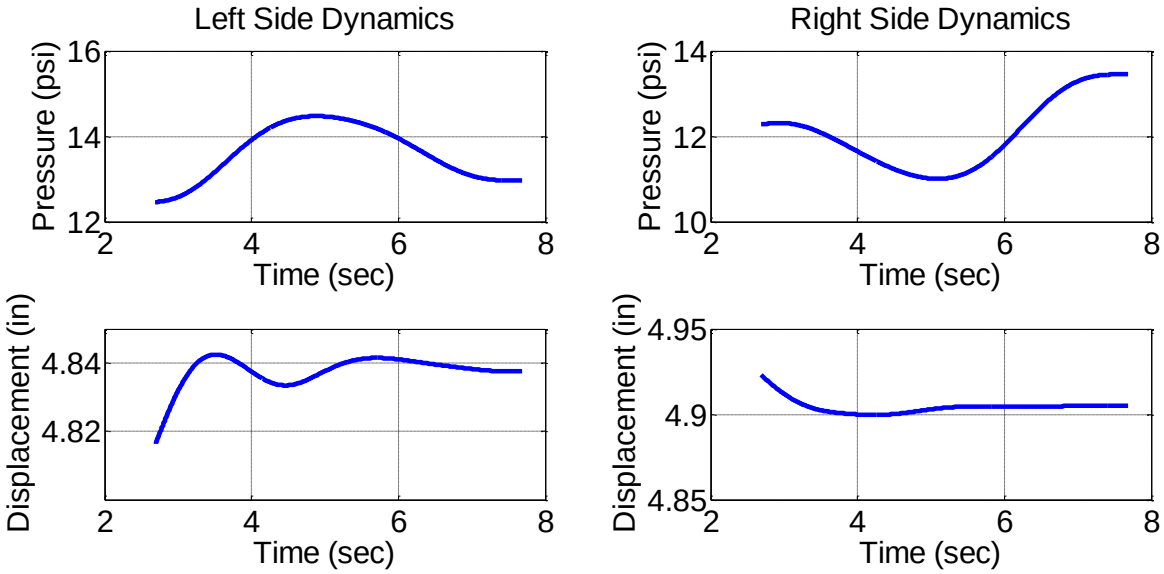

Figure 66. Plots of left and right side dynamics

5.2 Summary and Conclusions

The flow characterization analysis and testing of different generic load-leveling valves were provided in this study, followed by a systematic approach to redesign an enhanced disk/slot valve. The new design provides a simple, cost-effective, load-leveling solution that supplies large air flow rate, while it also maintains a fast dynamic response. The new valve has only one moving component, and unlike the chambered valve, it is compact and can be easily integrated with various suspension setups.

An innovative experimental approach was introduced to precisely estimate the mass flow rate of a load-leveling valve under different pressure conditions without implementing a mass flow meter. A series of dynamic airspring tests was then conducted, and the flow behavior of the system was validated by the force-displacement responses of the air spring due to various displacement excitations by using a common heavy-truck pneumatic suspension. The introduced valve flow measure can be effectively incorporated in future pneumatic systems modeling and development.

A detailed flow curve reshaping and redesign of the disk/slot valve process were discussed through precise metering of the orifice area and lever arm length optimization. The results showed that the transient portion of the flow characterization curves indicated that the prediction was accurate in terms of air mass flow rate with a minimum amount of error. This level of error is inevitable considering the available dimensional tolerances in manufacturing processes, and uncertainties of the instrumentations and experimental setups. The experiments indicated that the chambered valve and the improved disk/slot valve yield hysteresis loops with very similar shape and resultant force values.

The findings of this study revealed the potential of the enhanced disk/slot load-leveling valve design in providing larger air flow rates at faster response times. Further testing and study, however, is needed to improve the current design in order to achieve better transient dynamics of the heavy truck air suspension.

5.3 Recommendations for Future Studies

Although the research presented in this thesis proved that the newly-designed disk/slot load-leveling valve is able to provide larger flow rates and faster response times than the existing designs, it is suggested that further investigation be conducted to establish the pros and cons of the design. In particular, it is recommended that effect of orifice shapes on the flow characteristics be determined. In this study, the flow coefficient was considered to be constant. The effects of a variable flow coefficient can be studied.

Additionally, a more in-depth study is needed to discover the optimal flow characterization curve that is applicable to different heavy truck suspension configurations. Specifically, it is recommended that the study be coupled with a complete pneumatic suspension system from the air tank to airsprings. The influences of all other components that are used in air suspension should also be considered. Likewise, the role(s) of load-leveling valve mechanism in the pitch, roll, heave, and unsprung mass dynamics of the front and dual rear axles could also be established in an additional study.

References

1. White, D.L., *Parametric study of leveling system characteristics on roll stability of trailing arm air suspension for heavy trucks*. 2000, SAE Technical Paper.
2. Presthus, M., *Derivation of air spring model parameters for train simulation.* Master's Thesis, Department of Applied Physics and Mechanical Engineering, Division of Fluid Mechanics, LULEA University, 2002.
3. Elbeheiry, E.M., et al., *Advanced ground vehicle suspension systems-a classified bibliography.* Vehicle System Dynamics, 1995. 24(3): p. 231-258.
4. Robinson, W.D., A.G. Kelkar, and J.M. Vogel. *Modeling and Identification of a Pneumatic Air Spring-Valve-Accumulator System for Semi-Active Suspension Control*. in *ASME 2012 5th Annual Dynamic Systems and Control Conference Joint with the JSME 2012 11th Motion and Vibration Conference*. 2012. American Society of Mechanical Engineers.
5. Hendrickson, T.W.R.O.U. *Height control valves*. [cited 2016 January 15]; Available from: http://www.hendrickson-intl.com/Trailer/On-Highway/Height-Control-Valve. .
6. Sreedhar, B. and C. Deshmukh, *A Simplified Model of Air Suspension for Multi Body Simulation of the Commercial Passenger Vehicle*. 2013, SAE Technical Paper.
7. Reitz, V., *Valves Keeps Trucks On the Level*, in *Machine Design*. Jul 11, 2002. p. 39.
8. Hadley. *500 Serise Valve*. [cited 2016 February 2]; Available from: http://www.hadleyadvantage.com/products-and-solutions/products/valves/500-series-valve. .
9. Trudeau, C.A., et al., *Leveling valve for air springs*. 1996, Google Patents.
10. Prabhakar, N., et al., *Theoretical and Experimental Investigation of Flow Rate of Leveling Valve with Filters for Different Operating Angles*. 2013, SAE Technical Paper.
11. L, H.O. and S.D. S, *Air spring system and damped air valve*. 1975, Google Patents.
12. Haldex. *Height control valve*. [cited 2016 February 17]; Available from: https://www.haldex.com/en/na/suspension-controls/height-control-valve/cr-height-control-valve/90054007/. .
13. NORGREN. *Lift Axle Control Module 5040 Series* [cited 2016 March 4]; Available from: https://www.dsuban.com/files/5040_Lift_Axle_Control_Module-1.pdf. .

14. Nakajima, T., et al., *Air suspension system model coupled with leveling and differential pressure valves for railroad vehicle dynamics simulation.* Journal of Computational and Nonlinear Dynamics, 2014. 9(3): p. 031006.
15. Quaglia, G. and M. Sorli, *Air suspension dimensionless analysis and design procedure.* Vehicle System Dynamics, 2001. 35(6): p. 443-475.
16. Lee, S., *Development and analysis of an air spring model.* International Journal of Automotive Technology, 2010. 11(4): p. 471-479.
17. Hao, L. and L. Jaecheon. *Model development of automotive air spring based on experimental research*. in *2011 Third International Conference on Measuring Technology and Mechatronics Automation*. 2011. IEEE.
18. Nieto, A., et al., *An analytical model of pneumatic suspensions based on an experimental characterization.* Journal of Sound and Vibration, 2008. 313(1): p. 290-307.
19. XU, X., et al., *Dynamic Modeling and Characteristic Simulation of Charging-discharging System for Electronically Controlled Air Suspension [J]*. Journal of System Simulation, 2011. 6: p. 032.
20. Bao, W., et al., *A study on dynamics model for coupled air springs suspension system.* Automotive Engineering, 2008. 30(3): p. 231-234.
21. Kim, H. and H. Lee, *Height and leveling control of automotive air suspension system using sliding mode approach.* IEEE Transactions on Vehicular Technology, 2011. 60(5): p. 2027-2041.
22. Moshchuk, N., Y. Li, and S. Opiteck, *Air Suspension System Model and Optimization*. 2011, SAE Technical Paper.
23. Barksdale. *52321 Serise Air Suspension Valve*. [cited 2015 November 19]; Available from: http://www.barksdale.com/en/products/datasheet/310/air-suspension-valve---52321-series/.
24. FLEXIM. *Technical Specification FLUXUS G608-F2*. [cited 2016 February 15]; Available from: http://www.flexim.com/sites/default/files/public_downloas/tsfluxus_g608xx-f2v2-1en_leu.pdf.

25. Instruments, S. *Fast Response High-Performance Immersible Thermal Gas Mass Flow Meter*. [cited 2016 February 20]; Available from: http://www.sierrainstruments.com/userfiles/file/datasheets/technical/620s-datasheet.pdf.
26. Honeywell. *Installation Instructions for PX2 Series Heavy Duty Transducers*. [cited 2015 December 5]; Available from: http://sensing.honeywell.com/honeywell-sensing-px2-series-heavy-duty-pressure-transducers-installation-instructions-50052336-8-en2.pdf.
27. Honeywell. *Hall-effect Rotary Position Sensors: RTY Series with Integral Actuator and RTP Series with External Actuator*. [cited 2015 December 5]; Available from: http://sensing.honeywell.com/honeywell-sensing-rty-series-rtp-series-datasheet-32307665-b-en.pdf.
28. MTS. *Roehrig 2K EMA electromagnetic actuator* [cited 2015 October 17]; Available from: http://roehrigengineering.com/products/electro-magnetic-actuators/2k-ema/.
29. MTS. *Roehrig SHOCK Test Control and Damper Analysis Software*. [cited 2015 October 18]; Available from: http://roehrigengineering.com/products/dyno-software/.
30. TRANSLATION, D. *DT9816 Series Low-Cost Simultaneous DAQ*. [cited 2015 November 4]; Available from: http://www.datatranslation.com/Products/Low-Cost-DAQ/DT9816.
31. Chen, Y., M. Ahmadian, and A. Peterson, *Pneumatically Balanced Heavy Truck Air Suspensions for Improved Roll Stability*. 2015, SAE Technical Paper.
32. Smith, C.W., *Calculations of Flow of Air and Diatomic Gases.* Journal of the Aeronautical Sciences, 2012.
33. Weisstein, E.W.a.M.-.-A.W.W.R. *Circular Segment* [cited 2016 June 16]; Available from: http://mathworld.wolfram.com/CircularSegment.html.